ADDIS ABABA UNIVERSITY

ADDIS ABABA INSTITUTE OF TECHNOLOGY

SCHOOL OF CIVIL AND ENVIRONMENTAL ENGINEERING

OPTIMIZED USE OF SETTLEMENT REDUCING PILES FOR RAFT FOUNDATION ON CLAY SOIL

A Thesis in Geotechnical Engineering

By Dawit Baye

11/10/2020

Addis Ababa

A Thesis

Submitted in Partial Fulfillment of the Requirements for the Degree of Master of Science

ADDIS ABABA UNIVERSITY

ADDIS ABABA INSTITUTE OF TECHNOLOGY

SCHOOL OF CIVIL AND ENVIRONMENTAL ENGINEERING

Optimized Use of Settlement Reducing Piles for Raft Foundation on Clay Soil

Submitted by:

Dawit Baye

Approved by the board of Examiners:

Dr.-Ing. Henok Fikre	_____	_____
Advisor	Signature	Date
Dr.-Ing. Samuel Tadesse	_____	_____
Internal Examiner	Signature	Date
Dr.-Ing. Tensay Geberemedhin	_____	_____
External Examiner	Signature	Date
Dr.-Ing. Mebruk Mohammed	_____	_____
Chair person	Signature	Date

Undertaking

I certify that research work titled "Optimized Use of Settlement Reducing Pile for Raft Foundation on Clay Soil" is my own work. The work has not been presented elsewhere for assessment. Where material has been used from other sources it has been properly acknowledged / referred

Dawit Baye

Acknowledgment

I am indebted to my convivial advisor Dr.-Ing. Henok Fikre for his unlimitted support and valuing the effort made during the study.

Abstract

In this study, a concept of using piles for settlement control has been examined through a Finite Element modeling technique. A raft alone may be adequate in terms of bearing capacity but predicted settlement may exceed tolerable values. Hence, piles may be provided under the raft foundation to make the system sound. The study begins with an analysis of an unpiled raft foundation to decide the requirement of piles followed by an extensive parametric study to optimize the pile usage through three-dimensional analysis. The results indicated that the differential settlement requirement can be meet with an increase in raft thickness but the vertical settlement increases in the same order. Vertical and differential settlement decreases with an increase in length and number of piles. For the considered loading and subsoil condition a central pile group area ratio of 26% reduced the differential settlement significantly and the corresponding load shared by the piles reach more than 40%. The pile spacing is an important parameter and the study shows a vertical settlement decreases with an increase in pile spacing owing to a reduction of interaction among piles while differential settlement increases with increasing pile spacing due to the stiffness reduction of the central portion of the piled raft in which maximum settlement is expected . The load sharing ratio increases with an increase in pile spacing. Strategic use of non-uniform pile length configurations, shorter piles at the center, and longer at edges, enhances the settlement performance of piles raft foundations for the same total pile length due to relatively longer piles at edges supports the cantilevered raft portion. Pile diameter variation shows no significant change in settlement values as the settlement increase associated with increase in pile diameter is compensated by the frictional resistance increase due to pile circumference frictional area increase. The effect of consolidation in the load sharing ratio reaches up to 14% along with its effect in increasing the settlement and hence the usual practice of pre-proportioning the super-structure load to the foundation units may not be the best solution as the long term behavior of these units will be altered due to consolidation.

Key words: Piled raft foundation, Finite Element modeling, Clay soil

Contents

List of Tables

List of Figures

Notations

$R_{total,s}$ - settlement dependent total resistance of pile and raft

$R_{raft,s}$ - settlement dependent resistance of raft

$R_{pile,k,j}$ - settlement dependent resistance of pile

α_{pr} - piled raft coefficient

S_{max} - maximum settlement

S_{min} - minimum settlement

ΔS -differential settlement

δ - angular distortion

K_{rs} -raft soil flexibility

$W(p)$ - total vertical displacement

ρ_i-soil displacement at typical element i

α_r - interaction factor

R_G - group reduction factor

α_{cp} -cap pile interaction factor

α_{pc} - pile cap interaction factor

σ_{ii}-normal stress

σ_{ij} -shear stress

ϵ -strain

D- stress-strain matrix

E - modulus of elasticity

E_{50} - reference stiffness modulus at confining pressure (p^{ref})

E_{ur} - reference unloading stiffness modulus at confining pressure (p^{ref})

E_{oed} - oedometer stiffness modulus

C' -effective cohesion

ϕ' -effective angle of internal friction

m -stress level dependency factor

R_{inter}- interface reduction factor

R_f-failure ratio

ν- poisson's ratio

ψ - dilatation angle

e_{int} - initial void ratio

k_o^{nc} -lateral earth pressure

k_x, k_y -permeability coeeficients

Abbreviations

$SRPs$ -settlement reducing piles

FEM- finite element modeling

$2D$ - two dimensional

$3D$ - three dimensional

$GARP$ - geotechnical analysis of rafts with piles

$GASP$- geotechnical analysis of strips with piles

$FLAC$ -fast Lagrangian analysis of Continua

$APRILS$-analysis of piled raft in layers soils

Chapter 1

Introduction

1.1 Background

Foundation design followed by actual construction is a vital step in any Engineering project. The one-way nature and maintenance costliness (in some cases even not able) drive the motives of academicians and practitioners to give much emphasis to understand the behavior when it is subjected to artificial and natural phenomena and to come up with an optimized design recommendation and philosophies.

The common practice in foundation design is to assess the potential of using shallow foundations if reasonably supporting geologic medium exists near shallow depths or extending the foundation unit (pile) to a deeper strong stratum, all aim at providing safety, reliability, and serviceability to the structure by transmitting the load to the wider and stronger soil strata. However, combined use of both foundation types, shallow foundation (raft) and deep foundation (pile), will result in a better performance as the contribution of the bearing capacity of the raft, due to the contact pressure developed between the raft bottom and soil, is considered provided sound strata is located beneath the raft. The pile geometry and length will significantly be reduced owing to the bearing and settlement control performance of the raft, this results in a better economy.

As with any foundation system, the design of piled raft shall address issues such as ultimate load capacity, maximum total, and differential settlement for different types of loading conditions. Besides, the proportion of load carried by each interacting unit namely pile and raft shall be determined. Approximate analytical methods are developed but cannot adequately describe the behavior of piled rafts due to the three-dimensional complex interaction among the pile, raft, and soil. Hence, the numerical technique is believed to be a powerful tool to deal with this problem as advanced knowledge is being developed along with high-performance computing tools.

Where competent soil exists close to the ground surface, a combined pile and raft foun-

dation may provide the most economic form of foundation. Early analytical work by Butterfield and Banerjee (1971) suggested that, although the proportion of load taken by the piles would drop, the inclusion of a ground-contacting pile cap would have little effect on the stiffness of a pile group.

Mandolini et al. (2005) has suggested that piled rafts may be divided into two main categories:
1 'Small' pile groups, where the ratio or overall width B of the group to the pile length L is less than unity. Piles are needed to ensure adequate bearing capacity, and the pile cap (or raft) can easily be made sufficiently stiff to eliminate differential settlements. Even where the pile cap bears directly on the ground it will not contribute significantly to the overall performance of the foundation. 2 'Large' pile groups, with B/L ¿ 1, where the pile cap alone will usually provide sufficient margin against bearing failure and will contribute significantly in terms of transferring load directly to the ground. The design of such foundations hinges more on limiting the average and differential settlements to an acceptable level. Since for large rafts the flexural stiffness will be low, the location and length of any pile support should be chosen in order to minimize differential settlements.

From a simple approach to evaluating the overall stiffness of a piled raft, and assessing the load sharing between pile group and cap up to a more complex three-dimensional finite element analysis has been presented in this study.

1.2 Problem Statement

The demand for high-rise buildings is increasing and the associated increased structural load shall be adequately supported by the soil. Despite the adequate bearing capacity provided by the raft, the settlement criteria will deviate at least when the long term behavior of the soil is taken into account. This phenomenon was observed when the raft is founded on a typical clay profile considered in this study.

1.3 Objectives

The main objective of this study is to assess the feasibility of using a piled raft foundation on non-expansive clay soils and to investigate the contribution of added SRPs in the performance of the raft foundation. In the meantime, the study addresses the following specific objectives:

- Determining the settlement of raft foundation on settlement reducing piles
- Investigating the effect of additional piles support on total and differential settlement of the raft
- Determining the relative proportion of load carried by each foundation units before and after consolidation

1.4 Scope of the Study

The piling requirement study as a displacement control on non-expansive clay soils is limited to the uniformly distributed load acting on the foundation system.

1.5 Research Overview

The Second Chapter discusses and revises previous relevant theoretical, analytical, numerical, and experimental attempted design and analysis procedures to catch the important behavior of the piled raft foundation. The Third Chapter presents the input subsoil, pile, and raft material parameters along with the proposed constitutive behavior that governs them, and a numerical model of the problem constituents is developed using a Finite Element based software Plaxis 3D.

An extensive parametric study is presented and the results are discussed in detail in Chapter Four. Chapter Five concludes the study and points a recommendation for future study.

Chapter 2

Literature Review

2.1 Introduction

Piled Raft foundation analysis and design is essentially a soil-structure interaction problem. This involves the interaction between pile-soil, pile-raft, pile-pile, and raft-soil. Investigation on the foundation behavior and model development date back to the mid-twenties century. Zeevaert (1957) for the first time attempted to combine shallow and deep foundation for the compressible volcanic clay of Mexico City. The usual practice before was to provide a shallow foundation (Raft) and if it is not sufficient to withstand the entire structural load, a deep foundation (pile) will be provided. While Burland (1995) reports reveal an excessive settlement of the raft even though the foundation is far from a failure in bearing capacity. This points to the potential advantage of using piles for settlement reduction to satisfy the structural serviceability requirement.

2.2 Basics of Piled Raft Foundation

Piled rafts are usually favored for high rise buildings provided the sub-soil condition to comply with Poulos (2001) recommendations. These foundations utilize the advantage of both foundation units. According to the raft flexibility, the contact pressure developed between the raft and soil helps some part of the load to be shared significantly from the piles.

2.2.1 Load Bearing Behavior

Since foundation units are not limited to one, a piled raft foundation is expected to have the following basic interactions between the individual components.

- pile-soil interaction

- pile-pile interaction
- pile-raft interaction
- raft-soil interaction

These interactions are the major determinants of the bearing capacity and settlement behavior of the piled raft foundation. Figure 2.1 shows the interaction among foundation components of piled raft foundation.

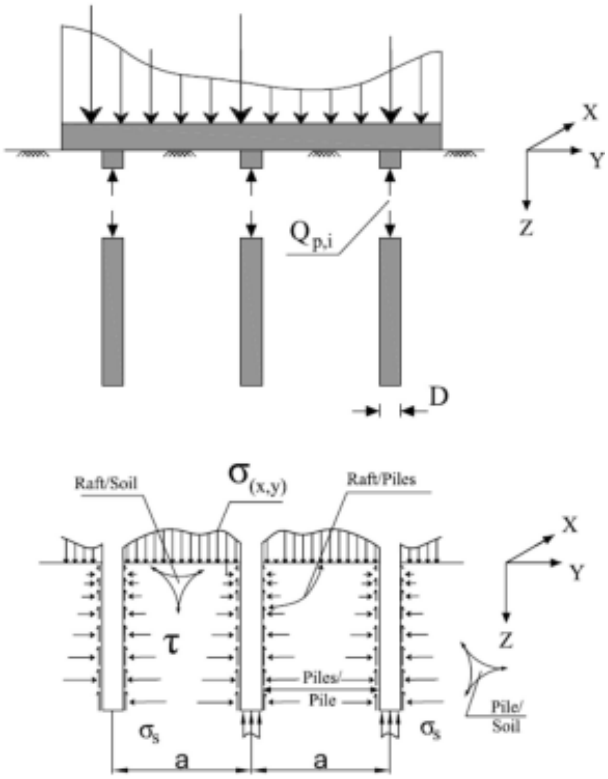

Figure 2.1: Interaction among foundation components of piled raft foundation

The settlement dependent total resistance offered is the sum of the resistance of the piles and the raft, or equivalently:

$$R_{total,k} = R_{raft,k}(s) + \sum R_{pile,k,j}(s) \tag{2.1}$$

The resistance of the raft can be determined by integrating the contact pressure developed over the raft soil area

$$R_{raft,k} = \int\int \sigma(s,x,y)dxdy \tag{2.2}$$

The resistance of the individual piles is computed as the sum of skin and base resistance:

$$R_{pile,k,j}(s) = R_{s,k,j}(s) + R_{b,k,j}(s) \tag{2.3}$$

The total external load is shared between the piles and the raft. The proportion of the load carried by the piles and raft is usually expressed using the piled raft coefficient α_{pr}, which is defined as:

$$\alpha_{pr} = \sum_{j=1}^{m} R_{pile,i} * \frac{1}{R_{total}} \tag{2.4}$$

The value of α_{pr} varies between 0 and 1, the two extremes representing the case of the unpiled raft and free-standing pile groups respectively.
An estimate of the vertical capacity of piled raft foundation has been suggested by Poulos (2001) as the smaller of:

- the ultimate capacity of the block containing the piles, plus that of the proportion of the raft outside the periphery of the pile group; and
- the sum of ultimate load of the raft and of all the piles in the system

2.2.2 Settlement Behavior of Piled Raft Foundation

According to the experimental evidence collected by Mandolini et al. (2005), the settlement of piled foundations be unnecessarily small. Thus there is room for further load while satisfying the serviceability requirement provided settlement prediction is reliable. Nowadays, the advent of computer technology helps a rigorous treatment of settlement problems.

The design of the piled raft foundation shall comply with local and international standards. The following settlement notations are used to deal with the serviceability of a building:

- Maximum settlement S: usually occurs at the midpoint of the piled raft foundation with piles of the uniform dimensions acted upon by uniform loads. In that case, its magnitude will be equal to the midpoint settlement S_M.

$$S_{Max} = S_M \tag{2.5}$$

- Minimum settlement S: usually occurs at the corner of the raft of piled raft foundation with piles of uniform dimensions acted upon by uniform loads. In that case, its magnitude will be equal to the corner settlement S_C

$$S_{Min} = S_C \tag{2.6}$$

- Differential settlement ΔS defined as the difference between the maximum and minimum settlements

$$\Delta S = S_{Max} - S_{MIn} \tag{2.7}$$

- Maximum angular distortion defined as the differential settlement between two points divided by the distance between them

$$\delta = \frac{\Delta S}{L} \tag{2.8}$$

The settlement of a piled raft foundation is a function of the stiffness and geometric parameters of the soil and foundation units. The dimensionless coefficient, called raft soil flexibility ratio K_{rs} defined by Horikoshi and RandolphHorikoshi and Randolph (1997), is used to describe raft flexibility.

$$K_{rs} = 5.57\frac{E_r}{E_s}\frac{1-{v_s}^2}{1-{v_r}^2}(\frac{B}{L})^{0.5}(\frac{t_r}{L})^3 \tag{2.9}$$

where:

K_{rs} raft soil stiffness ratio

E_r stiffness of the raft

E_s stiffness of the soil

$v_{s,r}$ poisons ration of soil and raft respectively

B width of the raft L length of the raft

t_r thickness of the raft

The flexibility is bounded by 0.008 and 54 for fully flexible and rigid cases as given by Reul and Randolph (2004). Sample stiffness ratio calculation for a typical raft thickness

of 0.7m is shown in Equation 2.10.

$$K_{rs} = 5.57\frac{E_r}{E_s}\frac{1-{v_s}^2}{1-{v_r}^2}(\frac{B}{L})^{0.5}(\frac{t_r}{L})^3 K_{rs} = 5.57\frac{35000}{45}\frac{1-0.3^2}{1-0.2^2}(\frac{15}{15})^{0.5}(\frac{0.7}{15})^3 = 0.417 \quad (2.10)$$

2.2.3 Advantages of Piled Raft Foundation

Piled raft foundations are useful in reducing the raft thickness necessary and result in an economical foundation system as shown by Love (2003). The other main advantages are summarized by Katzenbach et al. (1998) as:

- Reduction of heave caused during pit excavation
- Improvement of serviceability of shallow foundations by reducing settlements, differential settlement, and tilt
- Avoiding eccentricities by concentrating piles around highly loaded area
- Improvement of bearing capacity of shallow foundations making use of the load share of the raft
- Reduction of internal stresses and bending moments in the raft by an optimal arrangement of piles beneath the raft
- Reduction of the total number of piles in comparison to the conventional pile foundation

2.2.4 Design Philosophy

One of the principal benefits of casting a pile cap directly on the ground is enforcing a 'block' type failure. Franke (1991) observed the mode of failure of piles within a large group is extremely different from that of one pile, even the cap is suspended above the ground. Because of interaction effects, slip between the soil and the pile within a group will tend to begin at the base of each pile and progress upwards, instead of the other way around for one pile. If the pile cap acts directly on the soil surface, relative slip between pile and soil cannot occur at shallow depths, and therefore the ultimate limit state must involve punching failure of the whole block of soil containing the piles.

Three different design approaches are identified for piled rafts by Randolph (1994):

1. Conventional: where the foundation is designed essentially as a pile group, with regular spacing of the piles over the entire foundation area, but where allowance is taken into account for the load transmitted directly from the pile cap to the ground, primarily to ultimate load capacity.

2. Creep piling: piles are designed to operate at the working load at which significant creep starts to occur, typically 70-80% of the ultimate load capacity; sufficient piles are included to reduce the net contact pressure between the raft and the soil below the per consolidation pressure of the soil.

3. Differential settlement control: the piles are located strategically to reduce the overall average settlement substantially.

Also, there is a more extreme version of creep piling, in which the full load capacity of the piles is utilized: that is, some or all of the piles operate at 100% of their ultimate capacity. This gives rise to the concept of using piles primarily as settlement reducers, while recognizing that they also contribute to increasing the ultimate load capacity of the entire foundation system.

The load settlement behaviour of piled rafts designed according to the three design philosophies is depicted in Fig. 2.2.

curves reflection:
0 shows the behavior of the raft alone and an excessive settlement is observed at the design load.
1 represents a piled raft designed in a conventional way, for which the behavior of the piled raft is governed by the pile group behavior.
2 represents a creep piling where the piles operate at a lower factor of safety, but since fewer piles present, the raft is loaded more.
3 illustrate the system of using piles are settlement reducers in which the full capacity of the piles is utilized at the design load.
The design depicted in the curve 3 is favored in terms of economics.

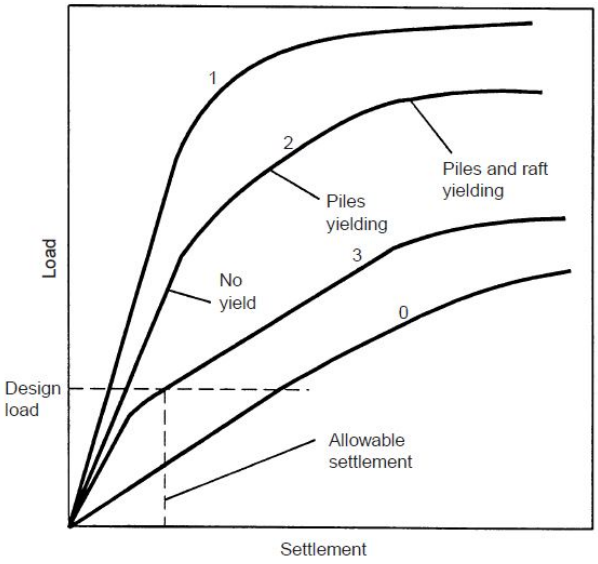

Figure 2.2: Load settlement curve for piled rafts according to various design philosophies (Poulos (2001))

2.2.5 Design Consideration

As of any foundation system, the design of a piled raft foundation requires the consideration of some issues. To provide an optimum foundation design, the following aspects shall be considered as indicated by Poulos (2001).

- Ultimate load capacity for vertical, lateral, and moment loading
- Maximum settlement
- Differential settlement
- Load shared between piles and raft
- Raft moments and shears for the structural design of the raft
- Pile loads and moments for the structural design of the piles

2.2.6 Design Process

The design process of the piled raft foundation consists of two stages. The preliminary stage assesses the feasibility of using a piled raft and the required number of the pile, to satisfy the design requirements. It involves the estimation of ultimate geotechnical

properties (vertical loading, lateral loading, moment loading), load settlement behavior, pile loads, raft moments, and shears.

The detailed design stage comes into effect when the preliminary design stage assures the feasibility of a piled raft foundation. This is performed to obtain the optimum number, location, and configuration of piles, and to compute the detailed distribution of settlement, bending moment, and shear force in the raft and piles. It involves the application of different models, geotechnical numerical methods, safety, and reliability analysis.

2.2.7 Favorable and Unfavorable Circumstances for Piled Raft

The most effective application of piled rafts occurs when the raft can provide adequate load capacity, but the settlement and/or differential settlement of the raft alone exceeds the allowable values. Poulos (2001) has examined several idealized soil profiles and has found that the following situations may be favorable.

- soil profiles consisting of relatively stiff clays
- soil profiles consisting of relatively dense sands

In both circumstances, the raft can provide a significant proportion of the required load capacity and stiffness, with the piles acting to 'boost' the performance of the foundation, rather than providing the major means of support. Conversely, some situations are unfavorable, including:

- soil profile containing soft clays near the surface
- soil profiles containing loose sands near the surface
- soil profiles that contain soft compressible layers at relatively shallow depths
- soil profiles that are likely to undergo consolidation settlements
- soil profile that is likely to undergo swelling movements due to external causes

In the first two cases, the raft may not be able to provide significant load capacity and stiffness, while in the third case, long term settlement of the compressible underlying

layers may reduce the contribution of the raft to the long terms stiffness of the foundation. Adequate precaution should be applied to consolidating and swelling soils.

2.3 Methods of Analysis

Several methods of analyzing piled raft have been developed, some of these have been summarized by Poulos (2000). Three broad classes of analysis method have been identified:

- Simplified calculation methods
- Approximate computer based methods
- Rigorous computer based methods

Simplified methods involve simple hand calculation using the theoretical solution for a raft and pile in the elastic continuum. Several simplifications are made on the behavior of soil medium and loading conditions.

The approximate computer-based methods are still based on elastic theory and two main approaches are presented by Poulos (2001)

2.3.1 Simplified Analysis Methods

Butterfield and Banerjee Approach

Butterfield and Banerjee (1971) were the first to estimate the load sharing between the pile and cap, and the corresponding settlement behavior for various pile configuration (pile number, size, and spacing) and cap type (contacting or floating). The analysis method adopted Mindlin's solution for a point load embedded in the interior of a semi-infinite elastic solid. By distributing such point load over the pile cap, an integral equation was developed for the vertical displacement of all points in the medium and expressed in terms of stress intensities (Fig. 2.3).

The analysis was on a small floating pile group with a rigid cap subjected to a point load in an elastic soil medium of semi-infinite depth. The total vertical displacement $W(P)$

due to a load of P can be expressed as:

$$W(p) = \int_c \phi_c K(P, Q_c) dC + \int_s \phi_s K(P, Q_s) dS \tag{2.11}$$

Where, the first portion of equation 2.11 gives the vertical displacement on the cap soil

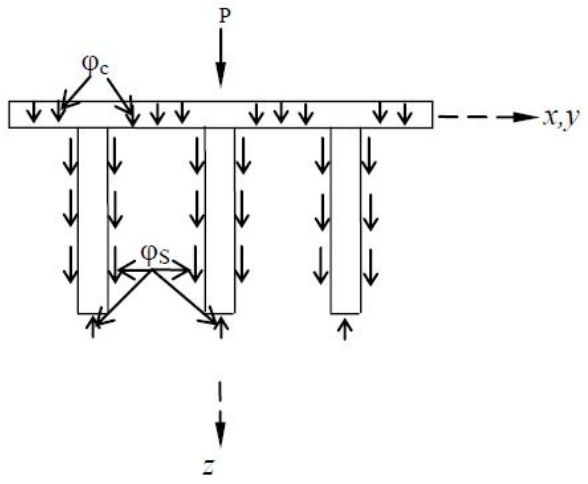

Figure 2.3: General arrangement of piled raft (butterfield and banerjee)

interface, due to the fictitious normal direct stress ϕ_c on element dC of effective cap area C (total cap area less area occupied by N piles). The second portion includes the vertical displacement due to fictitious shear and direct stress ϕ_s, acting at pile-soil interface of pile shaft element dS and base area (S). The terms K(P, Q_c) and K(P, Q_s) can be obtained from the Mindlin equation.

Davis and Poulos Approach

Poulos and Davis (1974) performed an elastic analysis of pile-raft interaction, considering soil as a semi-infinite elastic medium. The analysis is based on the interaction between two units, where, each unit consists of a rigid floating pile connected with a rigid circular cap, which is subjected to a point load. The rectangular or square mat would be the combination of such units covering the same area of the circular cap (Fig. 2.4). In this analysis, pile length is divided into 'n' cylindrical elements, each is subjected to a uniform shear stress p, acting around the surface, and the bottom circle is acted upon by a uniform vertical pressure p_b. The pile cap is also divided into 'v' annuli, each is uniformly loaded by vertical stress, p_c. The soil displacement at a typical element i is calculated from the

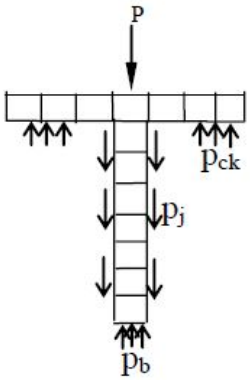

Figure 2.4: A single piled raft (butterfield and banerjee)

elastic stress-strain relationship as follows:

$$\rho_i = \frac{d}{E_s}(\sum_{j=1}^{n}({}_1I_{ij} + {}_2Iij)p_j + p_b({}_1I_{ib} + {}_2I_{ib} + \sum_{k=1}^{n} p_{ck}({}_1I_{ik} + {}_2I_{ik})) \tag{2.12}$$

Here, stress is expressed in terms of two groups of influence factors. One group $({}_1I_{ij}, {}_2I_{ij}, {}_1I_{ib}, {}_2I_{ib})$ is for vertical displacement due to point load in semi-infinite mass and it is calculated from Mindlin's equation. The other group of influence factors $({}_1I_{ik}, {}_2I_{ik})$ for vertical displacement, due to vertical displacement, due to surface load, is calculated by Boussinesq's equation.

where:

${}_1I_{ij}$, ${}_2I_{ij}$ are the influence factor for vertical displacement at i due to shear stress on element j of pile 1 and due to element j of pile 2 respectively

${}_1I_{ib}$,${}_2I_{ib}$ are the same at i due to vertical stress on base of pile 1 and 2 respectively.

${}_1I_{ik}$ is also the same at i due to uniform stress on annular k of pile 1 and ${}_2I_{ik}$ is due to element j of pile 2.

This analysis assumes incompressible pile and cap; hence the settlement of each element of a pile cap unit is the same. Again, since a free-standing pile is under consideration, the soil displacement is the same as that of the pile cap unit. Equation (2.12) is used to evaluate the settlement of two pile cap for various cap and pile dimensions and configuration. Another interaction factor, α_r, was introduced to generalize for various pile configuration as follows.

$$\alpha_r = \frac{\text{Additional settlement due to adjecent unit}}{\text{settlement of single pile}} \tag{2.13}$$

The above analysis can be used for any pile-raft system, considering the system consists of several pile-cap units, each having an equivalent circular cap area that would be occupied by the raft of a single pile. So, for a system comprises of m equivalent units. the settlement of a typical unit can be written by applying the superposition principle as:

$$\rho_i = \rho_1(\sum_{j=1, j\neq i}^{n} P_j \alpha_{rij} + P_i) \tag{2.14}$$

and the total settlement of the system can be given by, $\rho = R_G P_G \rho_1$

where:

α_{rij}=α_r of the equivalent pile cap unit

$$P_G = \sum_{j=1}^{n} P_j \tag{2.15}$$

$$\rho_1 = \frac{\rho_1}{R_e} \tag{2.16}$$

$$R_G = \frac{\text{settlement of the system}}{\text{settlement of single unit carrying same total load}} \tag{2.17}$$

ρ_1 is settlement of a free standing pile under unit load

ρ^- is the settlement of a single pile cap unit under unit load

R_G is a group reduction factor

The interaction factors are used to express the interaction between two independent pile-cap units and the stress around the pile shaft is considered uniform. However, the equivalent circular cap-pile unit concepts lack the accountability of the total integrated raft as a whole. The shear distribution around the equivalent cap periphery along with the bending moment effect is ignored. The structural integrity of the cap contributes to the shear redistribution to a greater extent. Load sharing between the foundation element is not explicit in the analysis and radial action is ignored. Application of Mindlin's and Boussinesq's equation remains the analysis procedure in the elastic regime. The load-displacement curve for the interaction of two rigid circular pile cap units was obtained first, and then these curves were superimposed to predict for all the pile cap units. However, this elastic superposition theory is valid, only when the piles are located along a circumference and subjected to the same load.

Randolph Approach

Randolph (1983) developed the simplest analysis method for a single pile cap unit and showed its applicability for a 3*3 piled raft foundation. The analysis was on a unit of the rigid floating pile, which is attached to a rigid circular cap and the soil was considered as elastic semi-infinite mass.

Based on the relationship between displacement,w_0, of pile shaft, and locally induced shear stress, τ_o, two pile cap interaction factors were developed.

$$\alpha_{cp} = 1 - \frac{ln(\frac{r_c}{r_o})}{\zeta} \tag{2.18}$$

$$\alpha_{pc} = \frac{r_c}{4L}[(1 - \frac{1}{2(1-\nu)} + (2 + \frac{1}{1-\nu})\sinh^{-1}(\frac{L}{r_c}))] \tag{2.19}$$

where:

α_{cp} is the cap pile interaction factor

α_{pc} is pile cap interaction factor

ζ include the influence of pile geometry and relative homogeneity of the soil after Randolph and Wroth (1978)

$$\zeta = \ln \frac{r_m}{r_o} \tag{2.20}$$

r_m is the maximum radius of influence of pile, which is related to the pile length as

$$r_m = 2.5\rho(1-\nu)L \tag{2.21}$$

The above two interaction factors were then applied to correlate the stiffness (k), settlement (w) and load (P) carried by pile and cap as shown in equation (2.22)

$$\begin{bmatrix} \frac{1}{k_p} & \frac{\alpha_{pc}}{k_c} \\ \frac{\alpha_c p}{k_p} & \frac{1}{k_c} \end{bmatrix} \begin{bmatrix} P_p \\ P_C \end{bmatrix} = \begin{bmatrix} w_p \\ w_c \end{bmatrix} \tag{2.22}$$

This analysis was for a rigid pile cap unit, therefore, $w_p = w_c$ and to satisfy the reciprocal theorem the above matrix is expected to be symmetric. Considering this approximation the above flexibility matrix (Equation 2.22) can be solved for the overall stiffness and load

sharing as:

$$k_{pc} = \frac{k_p + (1 - 2\alpha_{cp})k_c}{1 - \alpha_{cp}^2 \frac{k_c}{K_p}} \tag{2.23}$$

$$\frac{P_c}{P_c + P_p} = \frac{(1 - \alpha_{cp})k_c}{k_p + (1 - \frac{2\alpha_{cp}}{k_c})} \tag{2.24}$$

This elastic analysis can calculate only the total settlement of a single pile cap unit, with a direct estimation of load, carried by each component of the foundation. However. Randolph (1983) concluded that the above relation for stiffness, settlement, and load sharing is applicable for a large pile group of any size, where the equivalent cap radius is calculated from the raft area associated with each pile.

Fleming et al.,1992

This method combines the stiffness of the raft and foundation and introduces the stiffness of the piled raft foundation system. It is based on the principle and formula presented by Fleming (1992). The settlement of the system is divided into two components as a settlement due to a load carried by the raft and settlement due to the load carried by the piles.

- settlement due to the load carried by the raft

$$S_{raft} = \frac{P_{net}}{k_f} \tag{2.25}$$

$$P_{net} = (q * B * B) - (n * f_s * m) \tag{2.26}$$

$$k_f = \frac{k_p + k_c(1 - 2\alpha_{cp})}{1 - \alpha_{cp} \frac{k_c}{k_p}} \tag{2.27}$$

$$\alpha_{cp} = \frac{\ln(\frac{r_m}{r_c})}{\ln(\frac{r_m}{r_o})} \tag{2.28}$$

$$r_c = \sqrt{\frac{B^2}{n\pi}} \tag{2.29}$$

$$r_m = 2.5L\rho(1 - \nu) \tag{2.30}$$

where:

P_{net} net load

q pressure on the raft

B width of the foundation

n number of pile in the group

f_s shaft capacity

m percent of pile capacity mobilization

L length of pile in the group

r_o pile radius

ν poisson's ration of the soil

ρ soil inhomogenity factor

$$k_p = \frac{2\pi L G_L}{\ln(\frac{r_m}{r_o})} \tag{2.31}$$

$$k_c = \frac{2G_L}{I(1-\nu)}\sqrt{(B*B)} \tag{2.32}$$

where: I is influence factor for the raft

- settlement due to the load carried by the piles

$$S_{pile} = S_{elastic} * \alpha_{cp} \tag{2.33}$$

$$S_{elastic} = R_s * (slip) \tag{2.34}$$

where: R_s is settlement ratio

- Thus, the total settlement will be sum of the raft and pile settlement

Burland's Approach

The piles are expected to use their full capacity at the design load when they are intended for use as settlement reducers and Burland (1995) proposed a simplified design step (Fig. 2.5).

- Estimate the total long term load settlement relationship for the raft without piles. The design load P_o gives a total settlement S_o.
- Assess the acceptable design settlement S_d, which should include a margin of safety.
- P_1 is the load carried by the raft corresponding to S_d

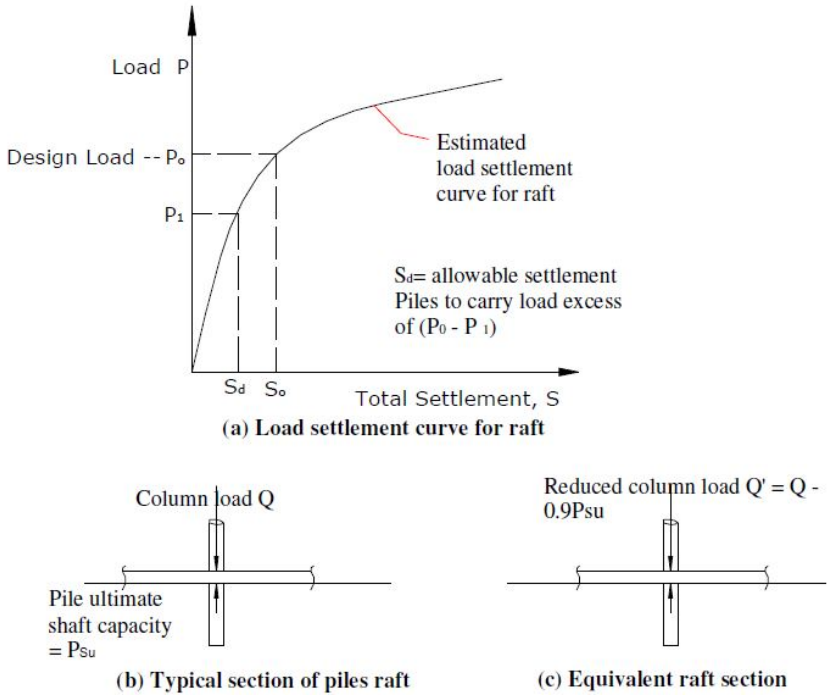

Figure 2.5: Burland's simplified design concept

- The load excess $P_o - P_1$ is assumed to be carried by settlement reducing piles. The shaft resistance of these piles will be fully mobilized and therefore no factor of safety is applied. However, Burland suggests that a "mobilization factor" of about 0.9 be applied to the "conservative best estimate" of ultimate shaft capacity, P_{su}.

- If the piles are located below columns that carry a load above P_{su}, the piled raft may be analyzed as a raft on which reduced column loads act. At such columns, the reduced load Q_r is:

$$Q_r = Q - 0.9P_{su} \tag{2.35}$$

- The bending moments in the raft can be then obtained by analyzing the piled raft as a raft subjected to the reduced load Q_r

- The process of estimating the settlement of the piled raft is not explicitly set out by Burland, but it would appear reasonable to adopt the approximate approach proposed by Randolph (1994).

$$S_{pr} = S_r * \frac{K_r}{K_{pr}} \tag{2.36}$$

where:

S_{pr} settlement of piled raft

S_r settlement of raft with out piles subjected to the total applied loading

K_r stiffness of the raft

K_{pr} stiffness of piled raft

2.3.2 Approximate Computer Based Methods

An approximate numerical analysis method in which the raft is presented by a series of strip footings and the piles are presented by springs of appropriate stiffness was developed by Poulos (1991). Approximate allowance was made for the raft-raft, raft-pile, pile-raft, pile-pile interactions (Fig. 2.6). For the practical purpose, this method was implemented with a computer program Geotechnical Analysis of Strip with Piles (GASP). Even if a reasonable agreement was obtained as compared to more complete analysis methods, it has limitations that it can not consider torsional moments within the raft. It may also not give consistent settlements if two strips in two directions through a particular point are analyzed.

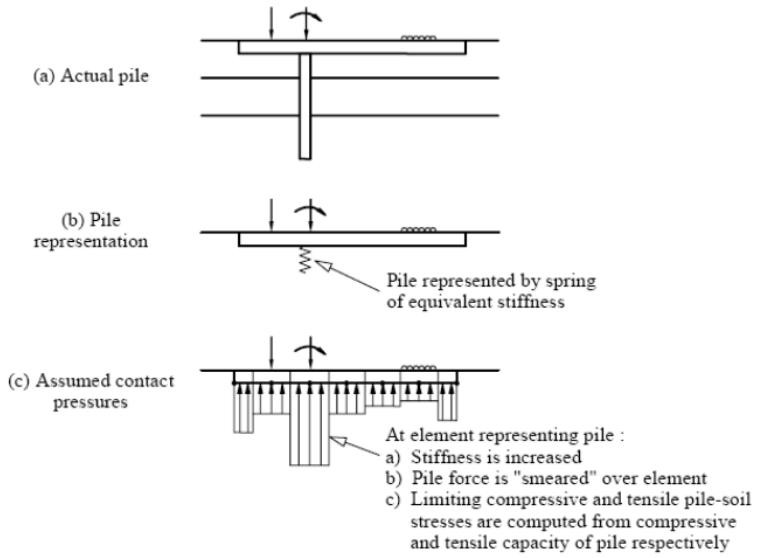

Figure 2.6: Representation of piled raft via GASP analysis

A hybrid approach in which the raft was modeled by two-dimensional thin plate finite elements whereas the piles were modeled by one-dimensional finite elements was formulated by Clancy and Randolph (1993).

Clancy and Randolph,1993

This method considers the interaction between pile and raft. The numerical representation of this method is depicted in Fig. 2.7. Moreover, like the other methods, the overall stiffness of the pile raft system is considered.

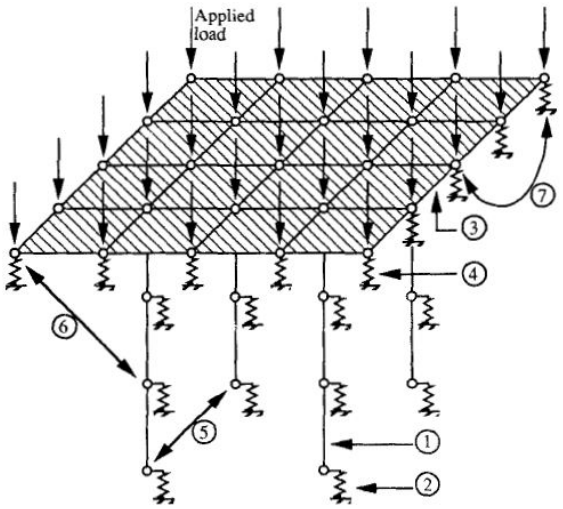

Figure 2.7: Numerical representation of piled raft

Notations:

1 One dimensional pile element

2 Ground resistance at each pile node represented by non linear $T - Z$ springs

3 Two-dimensional plate bending finite element raft mesh

4 Ground resistance at each raft node represented by an equivalent spring

5 Pile-soil-pile interaction effects calculated between pairs of nodes using Mindlin's equation

6 Pile-soil-raft interaction

7 Raft-soil-raft interaction

Thus the settlement is calculated as:

$$w_{pr} = \frac{P_t}{k_{pr}} \tag{2.37}$$

$$k_{pr} = \frac{[k_p + k_r(1 - 2\alpha_{rp})]}{[1 - (\frac{k_r}{k_p})\alpha_{rp}^2]} \tag{2.38}$$

$$\alpha_{pr} = \alpha_{rp}\frac{k_r}{k_p} \tag{2.39}$$

where:

n number of piles

d diameter of pile

$$k_p = \frac{2\pi L G_L}{\ln(\frac{r_m}{r_o})} \tag{2.40}$$

$$k_p = \frac{2G_L}{I(1-\nu)}\sqrt{(B*B)} \tag{2.41}$$

$$r_m = 2.5L\rho(1-\nu) \tag{2.42}$$

Furthermore, the values of α_{rp} and α_{pr} can be calculated again in order to check with previously calculated values

$$\alpha_{rp} = \frac{k_p}{p_p}(w_{pr} - \frac{p_r}{k_r}) \tag{2.43}$$

$$\alpha_{pr} = \frac{k_r}{p_r}(w_{pr} - \frac{p_p}{k_p}) \tag{2.44}$$

where:

p_r is load carried by the raft

p_p is load carried by piles

2.3.3 Rigorous Computer Based Methods

These include different computer-based methods ranging from the simplified two-dimensional methods to the more complex three-dimensional analysis methods. The rigorous computer-based methods give better results as compared to the simplified and approximate methods. Choice of an appropriate model and constitutive rules may even allow getting results close to theoretical solutions. The advent of more sophisticated software enables the use of finite element and boundary element methods for solving even complicated foundation problems more efficiently.

Prakoso and Kulhawy (2001) studied the behavior of piled raft foundation with a two-dimensional numerical method, the foundation is simplified as a two-dimensional model by handling it as a plane strain or as axially symmetric three-dimensional problems. In both cases, it would be difficult to model concentrated loads and piles as they will be smeared. Torsional moments in the raft can also not be determined. Also, Poulos (2001) observed that the two-dimensional analysis overestimates the settlement and pile loads because of

the plain strain assumptions. Thus it would be more practical to use three-dimensional analysis, especially for large scale projects.

Boundary Element Method

The boundary element method allows the analysis of the soil-structure interaction by considering the influence functions of the soil and the foundation plate. Only the boundaries of the foundation system need to be discretized with this method. And hence reduced calculation time and lower computer storage is required as compared to the finite element method. A study on the behavior of group piles in a homogeneous elastic soil has been made, in this analysis, the raft was assumed to be rigid and piles to be compressible. Kuwabara (1989) discretized the raft into a series of rectangular elements while the piles were discretized into a series of shaft and base elements.

Most of the analysis with the boundary element method considers linear elastic soil conditions. Even though it can also be applied to non-linear elastic or plastic models, the application of the soil structure contact is limited to the use of joint elements as observed by Franke et al. (1994).

Finite Element Method

The analysis and design of piled raft foundation are associated with complex soil-structure interactions, which require realistic modeling of the components, i.e., the structure and the soil inline with mechanical behaviors. With the advances in the field of computer engineering and the introduction of more powerful software, the finite element analysis has been getting more application for the design of geotechnical structures in the last four decades, The decrease in the computational time of such FEM analysis with the invention of high-speed computers is encouraging geotechnical engineers to apply it for solving complicated problems. Katzenbach et al. (1998) pointed out that three-dimensional finite element analysis is presently getting more applications in practice.

Finite Layer Method

Booker and Small (1986) developed a finite layer method to simplify three-dimensional problems to two-dimensional ones and hence to minimize computational efforts with the rigorous finite element methods. Since soil layers are usually layered horizontally, they can be treated as individual (finite)layers without discretizing into finite elements. Only the piles and raft are discretized using finite element methods. The application on piled raft subjected to both vertical and horizontal loads has been discussed by Small and Zhang (2002). Chow (2007) developed a computer program called APRILS which incorporates both the finite element and finite layer methods to model the structural elements and soil layer respectively.

2.4 Related Studies

A lot of research attempts have been made to grasp the key characteristics of the piled raft foundation in terms of load carrying and settlement behavior. Despite the various approach taken by the researchers, all agree on relative stiffness among the foundation components is the key parameter that affects the load sharing and settlement behavior of the piled raft foundation. The relative stiffness of the foundation again depends on the stiffness of the subsoil, dimension, and configuration of the foundation components.

Horikoshi and Randolph (1998) presented a new design concept in which piles are installed only beneath a central area of a relatively flexible raft to minimize the differential settlement. An approximate analysis procedure for the piled raft foundation proposed by Clancy and Randolph (1993) was used in the analysis. For raft rested on bearing soil, the unnecessarily suppressed settlement due to the installation of more piles than necessary results uneconomical foundation system which has been a common phenomenon for long when a conventional method of design is adopted. They demonstrated the potential advantage of a small pile group installed over the central area of the raft in minimizing differential settlements. The design concept is shown in Fig.2.8. The distribution of the contact pressure beneath a rigid raft on an elastic soil is well known, as illustrated in Fig 2.8a. If this contact pressure distribution can be deliberately generated beneath a flexible raft which is subjected to uniform loading, the differential settlement of the raft can be

reduced significantly. This can be achieved by installing a small pile group in the central area of the raft, reducing the raft contact pressure in that zone (Fig.2.8b). The study showed that piled rafts may be designed for negligible differential settlement by including a pile group over the central 16-25% (by area) of the raft, with the pile group stiffness approximately equal to that of the raft alone. The total pile capacity should be about 40-70% of the total applied load, depending on the group area ratio and the Poisson's ratio of the soil.

An extensive parametric study was conducted to study the influence of pile spacing, soil depth, pile compressibility, Poisson's ratio of the soil, and pile length. It was found that the average settlement was essentially independent of the pile spacing for given values of K_{rs} and L_p/a_{eq} and as the total applied load increases the differential settlement approaches that of the unpiled raft. Differential settlement of the piled raft on a soil layer with different thicknesses was essentially the same as that of an infinitely deep soil layer, even though the average settlement of the raft was smaller. The value of the differential settlement is essentially the same, irrespective of the Poisson's ratio of the soil, although the differential settlement shows a tendency to increase as Poisson's ratio decreases. The differential settlement is essentially the same, even if the pile length is changed significantly for the same K_{pr}.

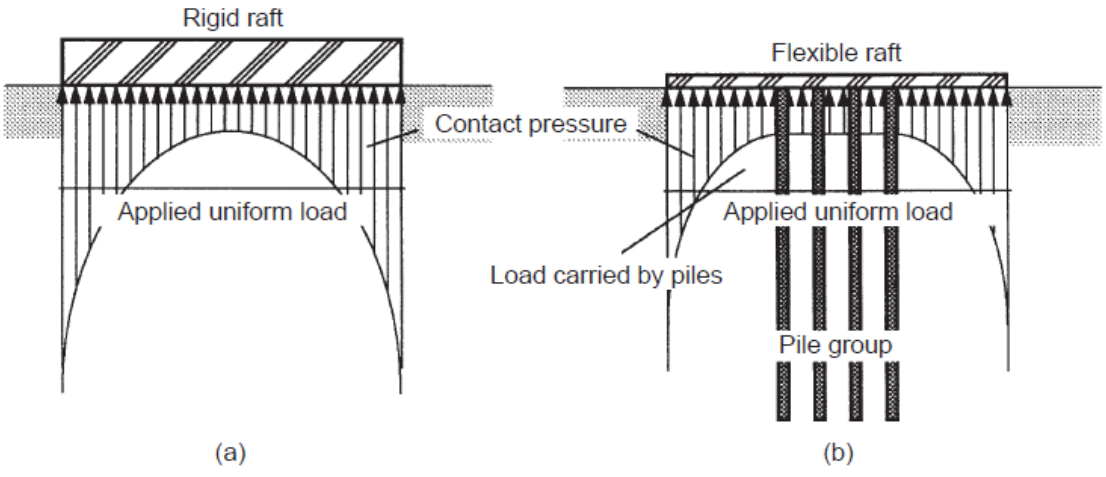

Figure 2.8: Principle of settlement reducing pile a) rigid raft b) flexible raft with small central pile group

3D numerical modeling of large piled raft foundation was developed to examine the settlement, load sharing, bending moment, and shear force behavior of piled raft foundation

on soft and stiff clay soil profiles by Mali and Singh (2020) . The Mohr-Coulomb constitutive model is used for the soil behavior and the interaction effects among the foundation units and the soil are accounted through the interface element. The effects of parameters such as pile spacing and raft thickness were studied. It was obtained larger pile spacing reduces the average settlement and enhance the load sharing coefficient while smaller pile spacing reduces the differential settlement. The present study includes the effects of other parameters such as pile length and diameter. Long term behavior due to consolidation is addressed as it is believed to occur in clay soil.

Leung et al. (2010) studied the benefit of using dis-similar pile length in free-standing pile group and piled raft design. The optimization study is applicable for frictional piles. A quadratic function is used to describe the pile length layout. It was obtained with the same total pile length, an optimized pile length configuration can both improve the overall stiffness of the foundation and reduce the differential settlement in free-standing pile group and piled raft design respectively. However, the pattern functions are limited to square pile groups and can not adequately represent the pile layout when pile numbers are increased significantly. The present study addresses an optimized benefit for non-squared pile raft.

Chapter 3

Methodology

3.1 Finite Element Modeling of Piled Raft Foundation

3.1.1 Introduction

From key aspects of soil behavior, elastic models are unlikely to be especially satisfactory except at lower load levels. If the material is assumed to be linearly elastic, then many of the details become uncomplicated (easy) and there are numerous existing solutions for the distribution of stresses and displacements in elastic systems that can be readily adapted, which were given by Poulos and Davis (1974). However, to handle nonlinear and history-dependent (elastic-plastic) material properties of soil, numerical analysis is almost definite to be required.

Our Focus is with the solution of field problems that we can state governing partial differential equations that describe how quantities of interest (field variables) must vary within a particular region and must satisfy boundary conditions at the edge of that region. We will concentrate particularly on problems of stress analysis where the quantities of interest are stresses and displacements but we might also concerned with other geotechnical field problems such as analysis of seepage flow (where the field variable is the pressure head) and the coupled flow and mechanical response that governs the consolidation process (where the field variables here combine pore pressure with stresses and displacements).

The steps involved in developing the numerical model can be depicted by the flow chart (Fig.3.1). The appropriate elastoplastic constitutive law for the soil continuum, the geometric modeling of the contact zone, and other parts along with the numerical step by step simulation, are major parts of the numerical model. The upcoming sections describe the steps involved in developing the model in PLAXIS 3D environment.

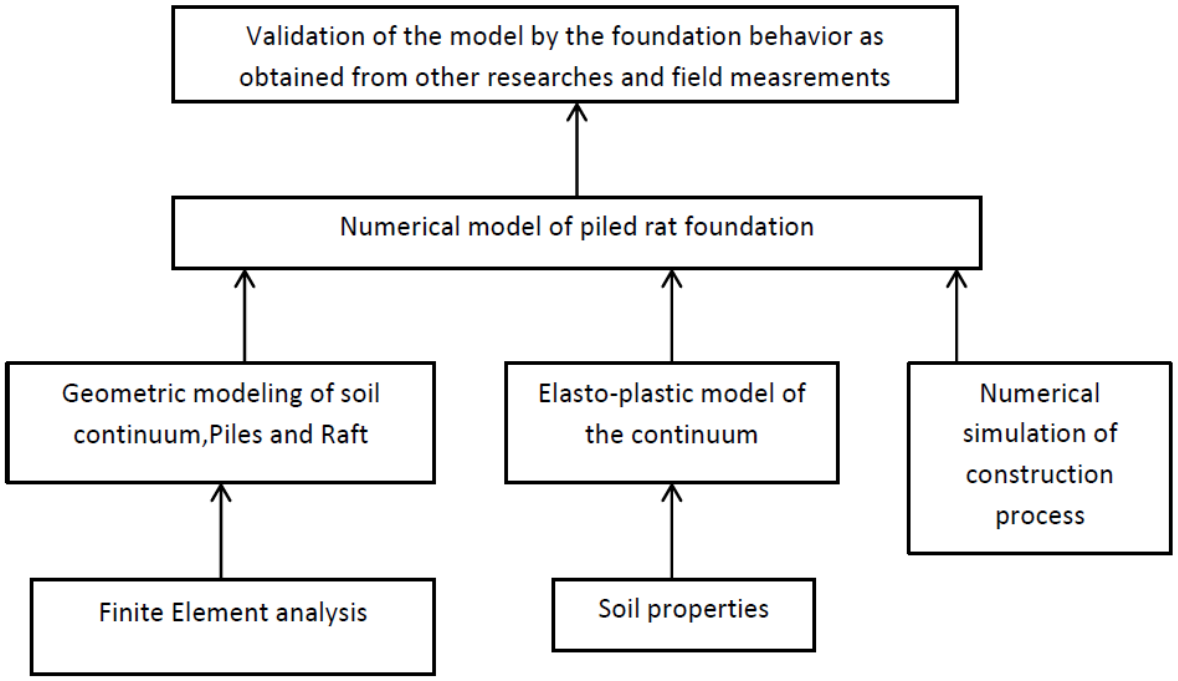

Figure 3.1: Numerical model development steps

3.1.2 Basic Considerations

Katzenbach et al. (1998) showed the Finite Element method is suitable for piled raft foundation analysis since it provides relatively realistic results as compared to the other methods discussed in chapter 2. The solution with this method should satisfy equilibrium, compatibility, and constitutive behavior pots. The boundary conditions which consider loads and displacements are also part of the requirements.

Equilibrium

To visualize and describe the equilibrium conditions of a soil mass, a typical three-dimensional element has been considered as shown in Fig.3.2. The different stresses have been labeled according to the chosen Cartesian coordinate axes x_1,x_2,x_3. Neglecting the inertia effects and all body forces, except the self-weight, stresses in a soil mass must satisfy the following three equations, as given by Timoshenko et al. (1951).

$$\frac{\partial \sigma_{11}}{\partial x_1} + \frac{\partial \sigma_{21}}{\partial x_2} + \frac{\partial \sigma_{31}}{\partial x_3} = 0$$

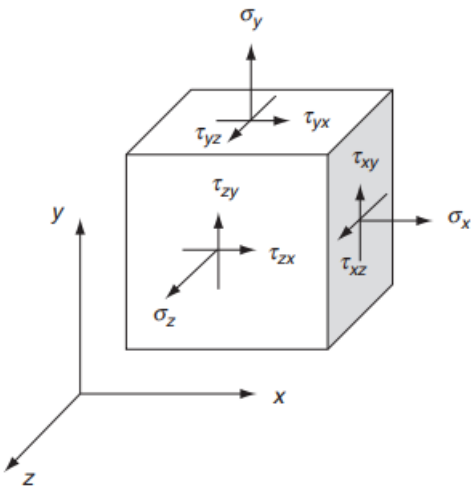

Figure 3.2: Stress on a typical 3D element

$$\frac{\partial \sigma_{12}}{\partial x_1} + \frac{\partial \sigma_{22}}{\partial x_2} + \frac{\partial \sigma_{32}}{\partial x_3} = 0$$
$$\frac{\partial \sigma_{13}}{\partial x_1} + \frac{\partial \sigma_{23}}{\partial x_2} + \frac{\partial \sigma_{33}}{\partial x_3} - \gamma = 0 \tag{3.1}$$

with:

σ_{ii} normal stress in the x_i direction

σ_{ij} shear stress along x_j relative to x_i direction

i and j indices with values 1,2 and 3

γ unit weight of the soil acting in x_3 direction

These equilibrium equations are in terms of total stress. For the fulfillment of boundary conditions the stresses at the boundaries must be in equilibrium with the applied surface traction forces.

Compatibility

Compatibility is a term used to describe the deformation of the Finite Elements used in the model. The compatibility of deformation involves no overlapping of material and no generation of holes. Fig.3.3 supports this physical (geometric) description of compatibility. The original plate elements are distorted after straining, forming the array shown in Fig.3.3. Incompatibility deformation, however, neither holes are created nor is any overlapping observed. Compatibility conditions are the geometrical relationships that strain tensor $\varepsilon_i i$ at each material point satisfy to ensure continuous deformation for the contin-

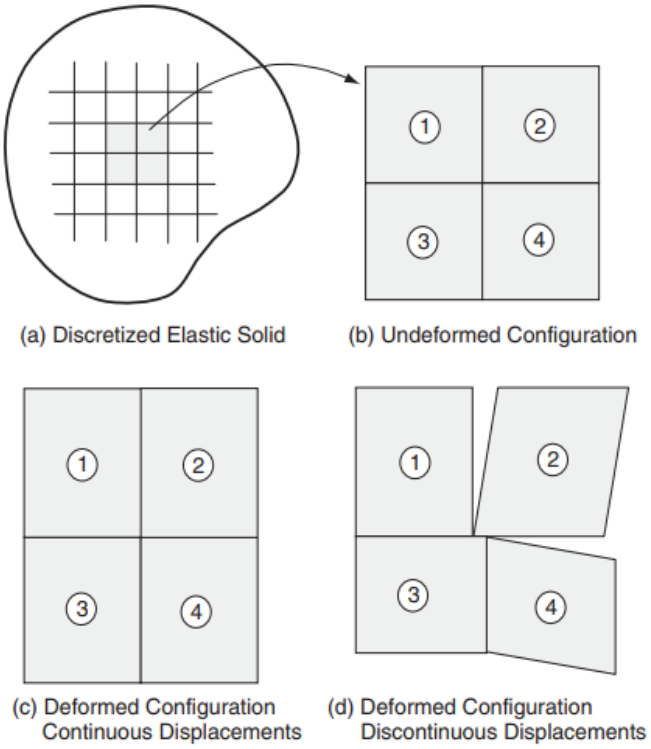

Figure 3.3: Modes of deformation of elastic solid

uum as a whole. This physical property can be described mathematically by considering strains of continuous deformation functions u, v, and w in the respective x_1, x_2 and x_3 axes as follows.

$$\varepsilon_{11} = \frac{\partial u}{\partial x_1}, \varepsilon_{22} = \frac{\partial v}{\partial x_2}, \varepsilon_{33} = \frac{\partial w}{\partial x_3}$$

$$\gamma_{12} = (\frac{\partial w}{\partial x_1} + \frac{\partial u}{\partial x_2}), \gamma_{23} = (\frac{\partial w}{\partial x_2} + \frac{\partial v}{\partial x_3}), \gamma_{13} = (\frac{\partial w}{\partial x_1} + \frac{\partial u}{\partial x_3}) \tag{3.2}$$

with:

ε_{ii} normal strain in the x_i direction

γ_{ij} shear strain along x_j relative to x_i direction

For compatibility displacement to exist. all the above components of strains and their derivatives must exist and be continuous to at least the second order. The displacement field must satisfy any specified displacements or restraints imposed on the boundary.

Constitutive Relations

The solution gap between fifteen unknown variables and nine equations, three equilibrium and six compatibilities, is filled by constitutive relations. This relation describes the

material behavior in terms of stress and strain relationships. The constitutive behavior can be expressed mathematically as:

$$\sigma = [D].\varepsilon \tag{3.3}$$

with:
σ - 6*1 stress matrix which is a simplified form of σ_{ii} and σ_{ij} described in Eq.3.3
$[D]$ - matrix which relates stress and strains, having 6*6 dimensions for linear elastic material and depends on elasticity modulus E and poisons ratio ν of the soil
ε - strain matrix which is a short form of ε_{ii} and γ_{ij} described in Eq.3.2
The behavior of the particular material varies with temperature, confining pressure, rate of strain, and other factors. However, under certain limited conditions, it is possible to idealize the soil as elastic, plastic, or viscous for the aim of stress and strain analysis. With this state of development of finite element computer programs almost unlimited range of solutions in soil mechanics is obtained. The material model applied during this study has been described in section 3.3.

Once the material constitutive law is established, the general formulation for the solution of a solid mechanics problem can be completed by applying the boundary conditions. For a soil mass acted upon by body Forces F_i and surface forces T_i, the system of equations form equilibrium, compatibility and constitutive laws can be combined to solve the 15 unknowns, namely 6 stresses, 3 displacements, and 6 strains. Figure 3.4 shows the inter-relationships of variables in the solution of a static solid mechanics problem. Equilibrium equations, compatibility equations and constitutive laws relates body and surface forces with stresses, displacements with strains and stresses with strain components respectively.

3.1.3 Formulation of Finite Element Method

The first step in solving numerical problems using Finite Element methods is setting the domain. Then discretization of the region under consideration into smaller elements called finite elements follows. The choice of appropriate element type and meshing technique has a major influence on the results of the numerical analysis. The mesh design must

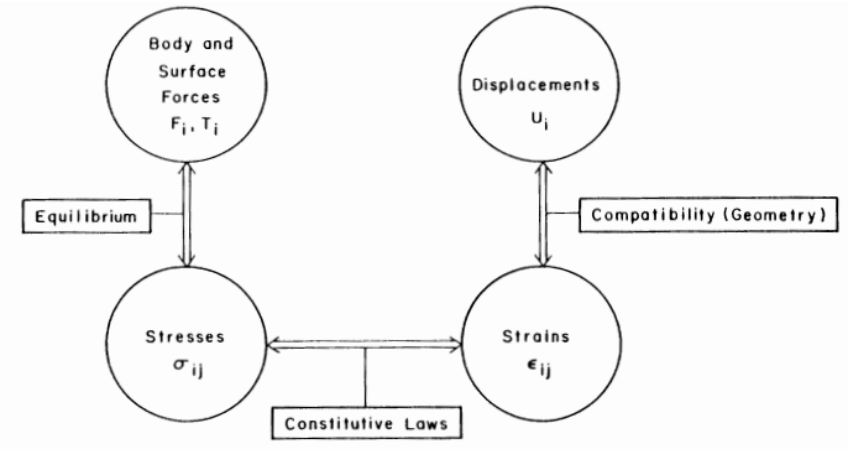

Figure 3.4: Interrelation ship of variables in the solution of a static solid mechanics problem (Chen et al. (1990))

take into account the boundary conditions, the material properties, and the geometry.

After the model is discretized, the primary variables shall be identified and rules as to how they vary over a finite element will be established. For geotechnical problems, displacements are usually taken as primary variables while stress and strains are taken as secondary variables. Over each element, the displacement components are assumed to have simple polynomial forms whose order depends on the number of nodes in the element. The displacement components are then expressed in terms of their values at nodes.

The equilibrium, compatibility, and constitutive conditions are then combined over each element to give element equations. For linear material behavior, the principle of virtual work is invoked on a kinematically admissible infinitesimal element with the assumption of very small displacements. This principle states that a deformable body remains in equilibrium if the works done by the internal and external forces are equal.

The separate element equilibrium equations are finally assembled to create a set of global equations. The assembly process is done by the direct stiffness method, where the terms of the global stiffness matrix are obtained by summing the individual element contributions taking into account the degrees of freedom which are common between elements. Finally, the boundary conditions (which include load and displacements) will be applied to the global equations and the large system of simultaneous equations will be formed. The resulting global equations will be of the form:

$$K.d = P \tag{3.4}$$

with:

K Global stiffness matrix derived from individual elements stiffness matrices

d Global displacement vector

P External force vector

This large system of simultaneous equations has to be solved to give nodal displacements u_i using different mathematical techniques. Most finite element programs apply the Gaussian elimination method, even though iterative techniques are usually adopted for three-dimensional problems. Once nodal displacements are obtained, strains and stresses will be evaluated using Equations 3.2 and 3.3.

Finite Element Mesh and Boundary Conditions

To perform Finite Element calculations, the geometry has to be divided into elements. A composition of finite elements is called a finite element mesh. The mesh should be sufficiently fine to obtain accurate numerical results. On the other hand, very finite meshes should be avoided since this will lead to excessive calculation times. The PLAXIS 3D program allows for a fully automatic generation of finite element meshes. The mesh generation process takes into account the soil stratigraphy as well as all structural objects, loads, and boundary conditions. The computations were carried out using the finite

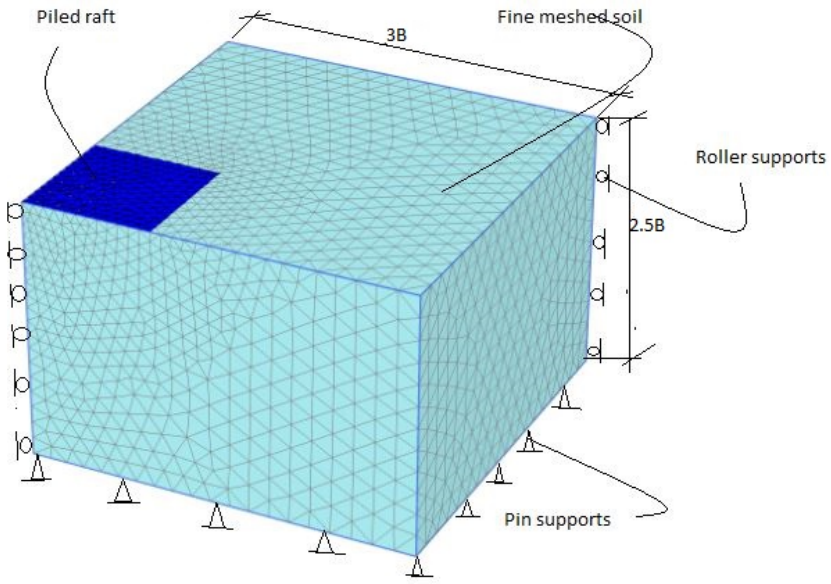

Figure 3.5: Finite Element Mesh(Fine)

element program PLAXIS 3D. A quarter symmetry 3D- numerical model with 10-noded elements is developed to investigate the behavior and study the optimized application of piled raft founded on clay soils.

The Finite Element mesh is shown in Figure 3.5, a relatively refined mesh is used near the structure to ensure accurate results.

1. The ground surface is free in all directions
2. Vertical model boundaries with their normal in the x-direction are fixed in the x-direction and free in y and z-direction
3. Vertical model boundaries with their normal in the y-direction are fixed in the y-direction and free in x and z-direction
4. The model bottom boundary is fixed in all directions

Sensitivity Analysis

To investigate the influence of the number of elements (mesh coarseness) on the settlement behavior of piled raft foundation, sensitivity analysis is performed. These were done by varying the element number (size) keeping material properties and all other parameters constant. The conducted analysis is given in Figure 3.6.

Element Type

The basic soil elements of the PLAXIS 3D finite element mesh are the 10-node tetrahedron elements (Fig. 3.7).
In addition to the soil elements, special types of elements are used to model structural behavior. For embedded beams, 3-node line elements are used, which are compatible with the 3-node edges of a soil element. In addition, 6-node plate elements are used to simulate the behavior of the raft. Moreover, 12-node interface elements are used to simulate soil-structure interaction behavior. The element formulations are given in the Appendix C.

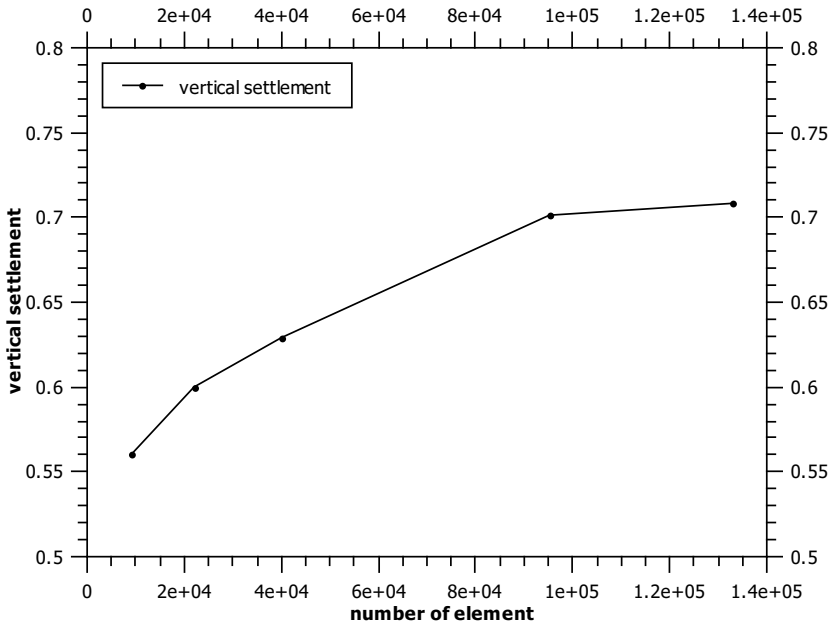

Figure 3.6: Sensitivity analysis

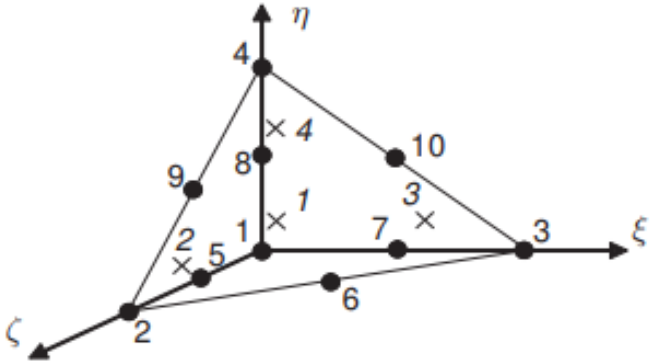

Figure 3.7: 3D soil elements (10-node tetrahedrons)

Loading

The considered load for piling requirement and parametric study are 150 kPa, uniformly distributed on top of the raft. This load is taken by the analogy of similar high rise building loads such as Torhaus der Messe founded on a similar soil profile considered in this study.

Constitutive Model

Advanced constitutive models have been formulated but the capability and shortcoming of these models are not always easy to work out, and the requirement for determination of parameters are not uniform. As a result, Lade (2005) pointed that determining an appropriate constitutive model for a particular task is difficult. The soil layer is simulated using the Hardening Soil model. This material model is considered as an advanced model for soil simulation, where the elastic deformation is represented by three input values instead of one value as in the case of the Mohr-Coulomb Model. The input moduli are the triaxial loading modulus, E_{50}, the triaxial unloading modulus, E_{ur},and the oedometer modulus, E_{oed} and can be calculated as:

$$E_{50} = E_{50}^{ref} \frac{(C'Cot\phi' + \sigma_3')}{C'Cot\phi' + P^{ref}} \tag{3.5}$$

$$E_{ur} = E_{ur}^{ref} \frac{(C'Cot\phi' + \sigma_3')}{C'Cot\phi' + P^{ref}} \tag{3.6}$$

Where:

E_{50} reference stiffness modulus at confining pressure (p^{ref})

E_{ur} reference unloading stiffness modulus at confining pressure (p^{ref})

C' and ϕ' effective shear parameters

m factor which represent stress level dependency of the stiffness: its value ranges from 0.4 to 1 depending on the type of the soil

The basic feature of the Hardening soil model as explained by Brinkgreve et al. (2013) is the stress dependency of soil stiffness and another potential advantage of this model in contrast to an elastic-plastic model is, the yield surface of hardening plasticity is not fixed in principal stress space, but it can expand due to plastic straining. This model contains shear and compression hardening. Shear hardening is used to model irreversible strains due to primary deviatoric loading while compression hardening is used to model irreversible plastic strains due to primary compression in oedometer loading and isotropic loading. The model parameters for Frakfurt clay used for this numerical study are given in Table 3.1 after Abdel-Azim et al. (2020). The relation between deformation moduli of hardening soil modulus and stress-strain relationship is shown in Fig.3.8.

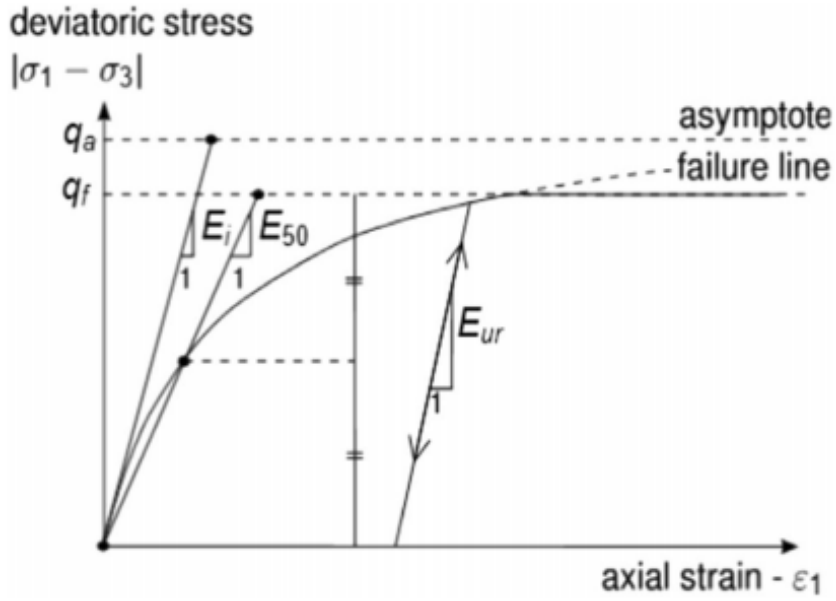

Figure 3.8: Relation between deformation moduli of hardening soil modulus and stress-strain relationship

The raft is modeled as 6-node triangular plate elements with 6 degrees of freedom per node: three translational degrees of freedom (U_x, U_y, and U_z) and three rotational degrees of freedom (ϕ_x, ϕ_y, and ϕ_z). The plate elements are based on Mindlin's plate theory. This theory allows for plate deflections due to shearing as well as bending. In addition, the element can change length when an axial force is applied.

Besides structural modeling of the raft, interfaces (joint elements) are added to plates to allow for proper modeling of soil-structure interaction Brinkgreve et al. (2013). They are used to simulate the thin zone of intensely shearing material at the contact between a plate and the surrounding soil. For this study, the interface material properties, which relate interface strength (wall friction and adhesion) to the soil strength (friction angle and cohesion), are assigned from adjacent soil property and a suitable value for the strength reduction factor (R_{inter}) is given in Table 3.1.

The pile is modeled as an embedded pile element (3-node line elements), which is a pile composed of beam elements that can be placed in an arbitrary direction in the sub-soil and that interacts with the sub-soil employing special interface elements. The interaction may involve skin resistance as well as foot resistance. The skin resistance and the tip force are determined by relative displacement between the soil and the pile. Although the embedded pile does not occupy volume, a particular volume around the pile (elastic zone)

Table 3.1: Material properties for numerical model

Material	Properties	Unit	Value
Soil	Unsaturated unit weight, γ_{unsat}	kN/m^3	20
	Saturated unit weight, γ_{sat}	kN/m^3	20
	Reference confining pressure	MPa	45
	at confining pressure, p^{ref}, E_{50}^{ref}		
	Plastic straining due to primary compression, E_{oed}^{ref}	MPa	45
	Elastic unloading reloading modulus, E_{ur}	MPa	90
	Poisson ratio, ν_{ur}	-	0.3
	Power,m	-	0.5
	Cohesion (undrained), C	kPa	100
	Cohesion, C'	kPa	20
	Angle of internal friction, ϕ	o	20
	Lateral earth pressure coefficient, k_o^{nc}	-	0.8
	Void ratio, e_{int}		0.6
	permeability,k_x, k_y	m/s	$1.4e-7$
	Dilation angle, ψ	o	-
	Failure ratio, R_f	-	0.9
	Interface reduction factor, R_{inter}	-	0.8
Pile and Raft	Modulus of elasticity, E	MPa	35000
	Poisson ratio, ν	-	0.2
	Diameter of pile,d_p	m	0.8
	Width of raft(square), B_r	m	15

is assumed in which plastic soil behavior is excluded. Brinkgreve et al. (2013) pointed that the size corresponds to pile diameter and the pile behaves almost like a volume pile .

Analysis Step

Simulation of the construction process using the FEM model requires a systematic choice and formulation of calculation steps representing the actual in-situ conditions. The analysis of piled raft is hence performed by using a stepwise simulation of the loading process. The following steps are used:

1. Initial stress condition:

   The in-situ stress state of the soil is simulated using a Ko procedure where the equilibrium of internal stresses and external loads is achieved.

2. Excavation for raft:

   Excavation of the soil above the foundation level is modeled by removing surcharge from the top of the raft.

Table 3.2: Geometric and material properties used in the validation of piled raft foundation after Poulos (2001)

Material	Properties	Unit	Value
Soil	Young's modulus,E_s	MPa	20
	Poisson's ration,ν_s	-	0.3
	Unit weight,γ	kPa	19
Raft	Young's modulus,E_r	MPa	30000
	raft length,L_r	m	10
	raft width,B_r	m	6
	raft thickness	m	0.5
Pile	Young's modulus,E_p	MPa	30000
	pile length,L_p	m	10
	pile diameter,D_p	m	0.5

3. Excavation for pile:

   The finite element volume of the pile space is deactivated.

4. Pile installation:

   The finite element volume of the pile space is reactivated.

5. Raft installation:

   The plate element representing the raft is reactivated.

6. Loading:

   The uniformly distributed load is applied on top of the raft.

3.1.4 Model Validation

A Finite Element Based software, PLAXIS 3D, is used to develop the piled raft model and it must be validated before the outputs are granted. Hence, to check the validity of the results two cases one a hypothetical model reported in American Society of Civil Engineers (ASCE) Technical committee - 18 (TC-18) and the other a 130m high Torhaus building with a total number of 84 bored piles with geometric dimensions 0.9m diameter and 20m length and a raft dimension of 17.5m * 24.5m is adopted. The raft lies 3m below the ground and has a thickness of 2.5m. The subsoil conditions and construction stages for Torhaus Der Messe are presented in Table 3.3 as given by Reul and Randolph (2003) The first considered model piled raft with soil, raft, and pile material and geometric properties are given in Table 3.2 are analyzed with PLAXIS 3D. From the total number of

Table 3.3: Step-by-step analysis of the construction process in the finite element analysis

Step	Applied load, P_{eff}:MN	Mean effective vertical stress at foundation level, $\sigma_{v'}$:kPa
In situ stress state	-	45
Excavtion to 3m below ground	-	0
Installation of piles	-	0
Application of weight of the raft as uniform load on subsoil(zero stiffness of raft)	26.8	62.5
Installation of raft	26.8	62.5
Loading of raft	200	466.5

Table 3.4: Previous and present study results of model piled raft

Model	Central settlement (mm)	Corner settlement (mm)
FLAC 2D poulos	65.9	60.5
FLAC 3D poulos	39.9	35.8
Poulos-Davis-Randolph	36.8	-
Geotechnical Analysis of Rafts with Piles(GARP)	34.2	26
Geotechnical Analysis of Strip with piles(GASP)	33.8	22
PLAXIS 2D after Omeman	32	26
PLAXIS 3D (present model)	28	22.4

nine piles, the middle three are subjected to a concentrated load of 2mN while the rest are subjected to 1mN. The result of the present numerical analysis and previous studies is summarized in Table 3.4. It gives 28 and 22.4mm central and corner settlements respectively. Despite some differences between the various method of calculation, the present study gives somewhat similar results.

Sommer (1991) reported the measured average settlement of 124mm while Reul and Randolph (2003) obtained a central settlement of 96mm. The present study with PLAXIS 3D gives a central settlement of 102mm which shows a close result with the measured value, which is 124mm. The typical Frankfurt clay soil parameters are used as given by Reul and Randolph (2003).

The present study with PLAXIS 3D gives a central settlement of 102mm which shows a close result with the measured value.

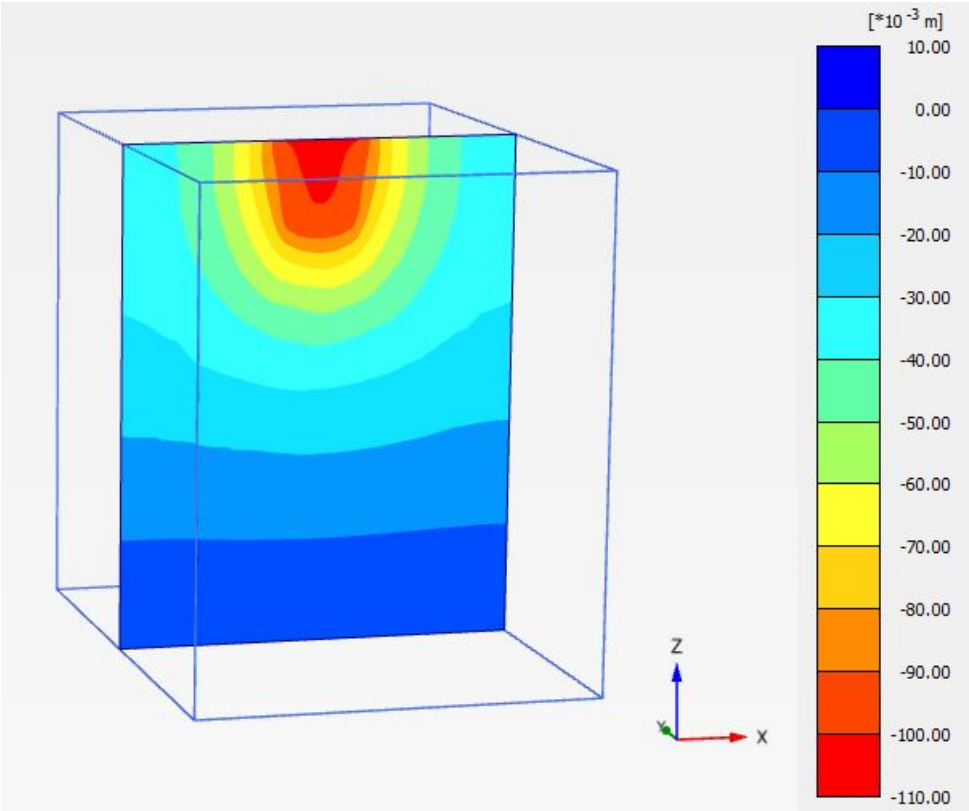

Figure 3.9: Torhaus der Messe output from FEM computation

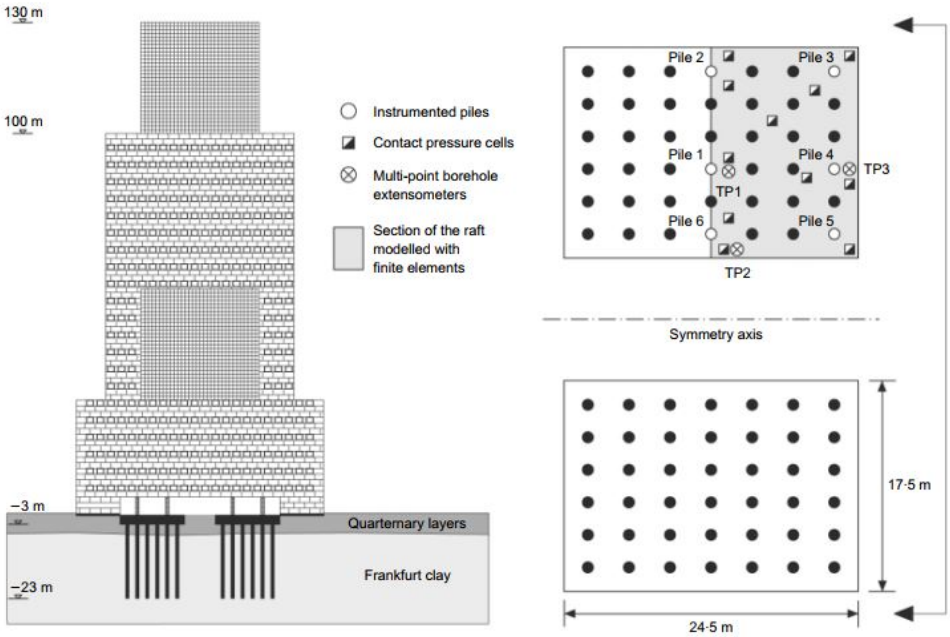

Figure 3.10: Torhaus building

Chapter 4

Settlement Based Design Optimization

Noting one of the aims of the present study is calling for a shift of capacity based analysis and design of piled raft to settlement based approach, the performance of unpiled raft foundation is investigated before adding the required number of piles to meet the design requirements. The problem is analyzed with FE based software PLAXIS 3D. Skempton and MacDonald (1956) suggests allowable settlement and distortion values after observing ninety-eight actual building performances. Following their attempt, Bowles et al. (1996) summarized a tolerable differential settlement for different foundation types and soil conditions. These values are given in Table A.1. The vertical settlements at raft center, corner, and edge are read from the output of the numerical computations and the foundation movement in-terms of settlement is limited to recommended values given by the above authors.

4.1 Unpiled Raft Behavior

A square raft with geometric dimensions 15m * 15m resting on a typical clay profile, having the pre-described subsoil condition given in Table 3.1, is shown in Fig.4.1. The hardening soil model is used to simulate soil behavior. This constitutive relation is favored as the total strains are calculated using stress-dependent stiffness, different for both loading and un-/reloading. The construction procedure is accounted for in Finite Element analysis as previously given in Sec 3.3.5.

As raft flexibility is a key parameter in vertical settlement analysis. it is carried out by varying raft thickness (Fig. 4.2). It can be observed from Fig. 4.1 that the vertical settlement shows a significant increase for raft thickness above 1.5m owing to the response of the soil to the subjected increased stress, whereas differential settlement decreases signif-

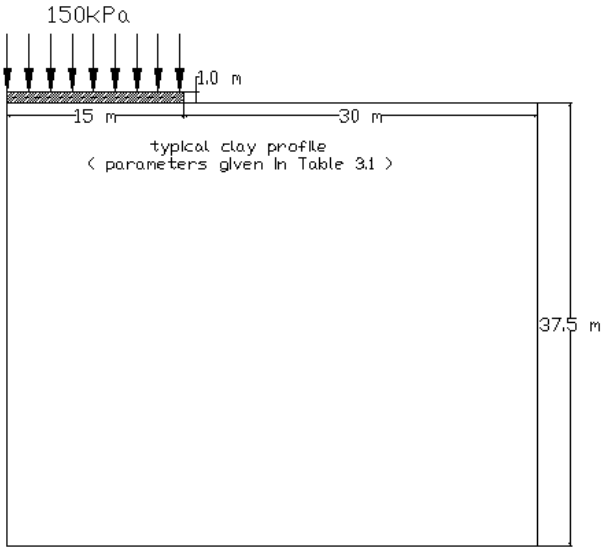

Figure 4.1: Raft geometry and loading condition

icantly up to a thickness of raft 1.5m which further shows a slight reduction owing to the rigid behavior of the raft. Gebregziabher and Achmus (2020) emphasized the raft should be flexible enough to interact with the piles and the soil. Flexibility calculations are done using the stiffness ratio defined by Horikoshi and Randolph (1997) as given in Eq.(2.9), and a sample calculation is made for a typical raft thickness and summarized in Tab. 2.1 for all other raft thicknesses. Reul and Randolph (2004) bound the flexible range from 0.008 - 54, which represents a perfectly flexible and fully rigid case respectively. A raft thickness of 0.7m is adopted for further calculations which lie within the recommended flexibility range as shown through Eq. 2.10.

As one expects, the maximum vertical settlement occurs at the center and a minimum at the corner (opposite vertices) of the square raft. The uneven settlement fashion of buildings causes more damage to structures than average vertical settlements, and hence this study aims at minimizing the differential settlement of the raft, and the allowable limits of the vertical and differential settlement are given in Appendix A.1.

Maximum vertical and differential settlement of 11.45cm and 7.9cm are obtained respectively and the angle of distortion value of 0.00372. The allowable values for maximum vertical and differential settlement and angle of distortion values for foundations on clay soils are 10cm, 4.5cm and 1/500 respectively as given by Bowles et al. (1996). The results of the Finite Element Model of the unpiled raft in-terms of the settlement are summarized in Table 4.1.

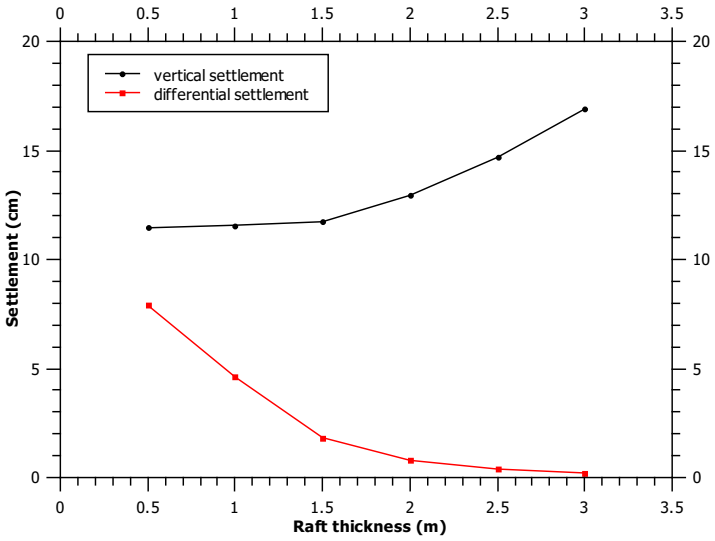

Figure 4.2: Vertical and differential settlement variation with raft thickness

Table 4.1: Unpiled raft settlements

Maximum vertical settlement (cm)	Minimum vertical settlement(cm)	Differential settlement (cm)	Angle of distortion(δ)
11.45	3.55	7.9	0.00372

Table 4.1 clearly shows the deviation of the computed results from the allowable values and hence, two options can be considered to tackle this problem. One is increasing the raft thickness so that the differential settlements will be suppressed, but at the expense of large bending moment due to raft thickness increase and higher vertical settlement. Second stiffening the central portion of the raft by introducing piles beneath the raft so that the differential settlement will be reduced. This study adopts the later option owing to the above discussed associated problems of increasing the raft thickness.

4.2 Piled Raft Behavior

Settlement reducing and load-carrying capacity of the piled raft when subjected to uniformly distributed load is studied with key variants including pile number, length, spacing, and diameter. For a flexible raft subjected to uniformly distributed loading conditions, the settlement behavior is as shown in Fig 4.3. Two important points are worth noting: one the soil which supports the raft edge will be tensioned, while the soil does not support tension, and second, the raft dishes in the center, which contribute to a signifi-

Table 4.2: Geometric properties for parametric study

Parameters	Unit	Value
Raft width,B_r	m	15
Raft length,L_r	m	15
Raft thickness,t_r	m	0.5, 1, 1.5, 2, 2.5, 3
Number of piles,n_p	-	1, 4, 9, 12, 15
Pile length,l_p	m	5,10,15
Pile spacing,S_p	m	3*, 4*, 5*
Pile diameter,d_p	m	0.8, 1, 1.5

$*$ denotes pile diameter

cant differential settlement increase. The location of piles is selected on the basis of the above-mentioned behaviors and thus at the center.

The settlement computations begin on a square raft having a dimension of 15m*15m by varying the thickness from 0.5 up to 3m. Then provide an adequate number of piles ranging from 1 -15, to achieve the settlement requirement after setting the thickness which makes the raft flexible enough to interact with the soil and piles. Each model with an adequate pile number obtained above is computed at three different pile lengths. Six computations to investigate the effect of pile diameter and spacing are then computed on twelve number of piles having a length of 15m.

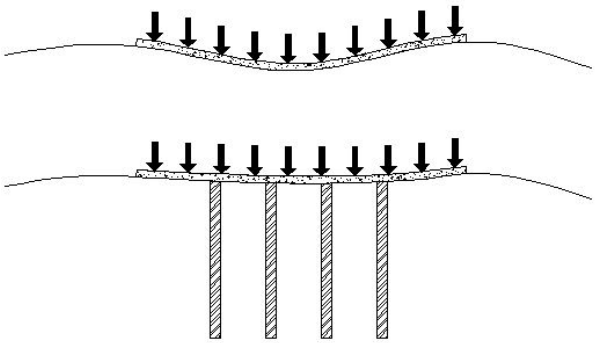

Figure 4.3: Raft subjected to uniformly distributed load (dished in the center)

4.2.1 Effect of number of piles

The plan view of the piles studied in this thesis is depicted in Fig. 4.4. The effect of the number of piles on maximum vertical and differential settlement behavior of piled raft foundation is shown in Figure (4.5,4.6).

Initially, a significant decrease in a vertical settlement is observed with an increase in pile number up to 9, then after the change in vertical settlement decrease is slight up to 12 piles. Further increase in pile number flattens the curve for the given loading condition. This behavior is attributed to the added pile support, which mainly derives its strength from friction.

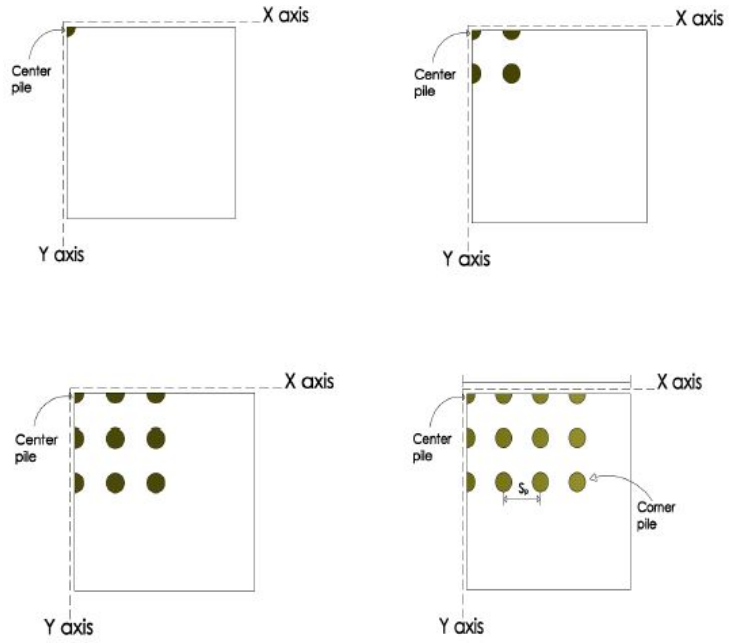

Figure 4.4: Plan view of the piles

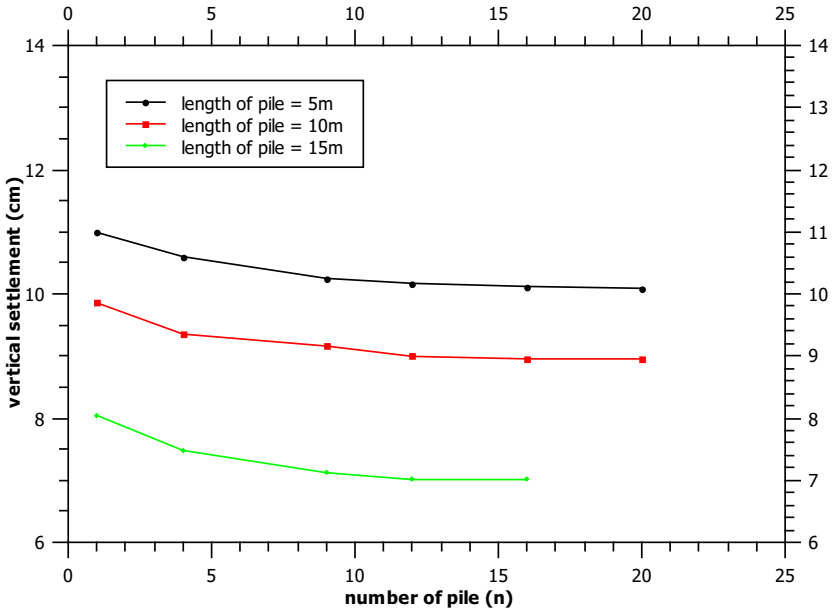

Figure 4.5: Vertical settlement variations with number of pile

Similarly, a continuous reduction in a differential settlement is observed with an increase in pile number up to 12 then a significant sudden drop in a differential settlement is seen for pile number above 12, this is because of stiffened central pile group. As differential settlement highly depends on the stiffness ratio of the central pile group area, in which higher settlement is expected, and near edges for uniform loading condition. The number of pile versus vertical settlement analyses helps in finding an optimum pile number corresponding to a minimum vertical settlement, for example, 12 for our loading condition. Apparently, the load carried by the pile increases with an increase in pile number.

Poulos (2001) elastic analysis of the effect of the number of a pile on maximum vertical, differential settlement and proportion of load shared by the piles for a 10 x 6m raft having a thickness of 0.5m subjected to concentrated and uniform load types shows a decrease in the maximum vertical settlement with an increase in pile number but becomes almost constant after a certain pile number. The present Finite Element study extends this study as it accounts for the non-linear behavior of soil and hence, it is an accurate method of design of piled raft foundation.

Reul and Randolph (2004) investigate the settlement performance of piled raft foundation subjected to non-uniform loading by considering four representative load patterns. Although the authors include piles at the periphery to support the heavily concentrated column loads located at raft edges, the potential advantage of using such configuration for uniformly distributed loads is seen in this study. For this pile configuration, the differential settlement is suppressed almost entirely, less than 1cm. Depending on the purpose of the structure this load configuration is helpful otherwise we can play on the allowable differential settlement values without suppressing the differential settlement entirely.

4.2.2 Effect of pile length

A basis piled raft model consisting of 12 piles with a spacing of three times the pile diameter is used to study the effect of pile length on settlement and load sharing behavior of piled raft foundation. Three different lengths of piles i.e 5m, 10m, and 15m are used. These effect on maximum vertical and differential settlement behavior of piled raft foundation is shown in Figure 4.5 and 4.6 respectively. For a given number of piles, a similar decrease trend in a vertical and differential settlement with pile length is observed. The

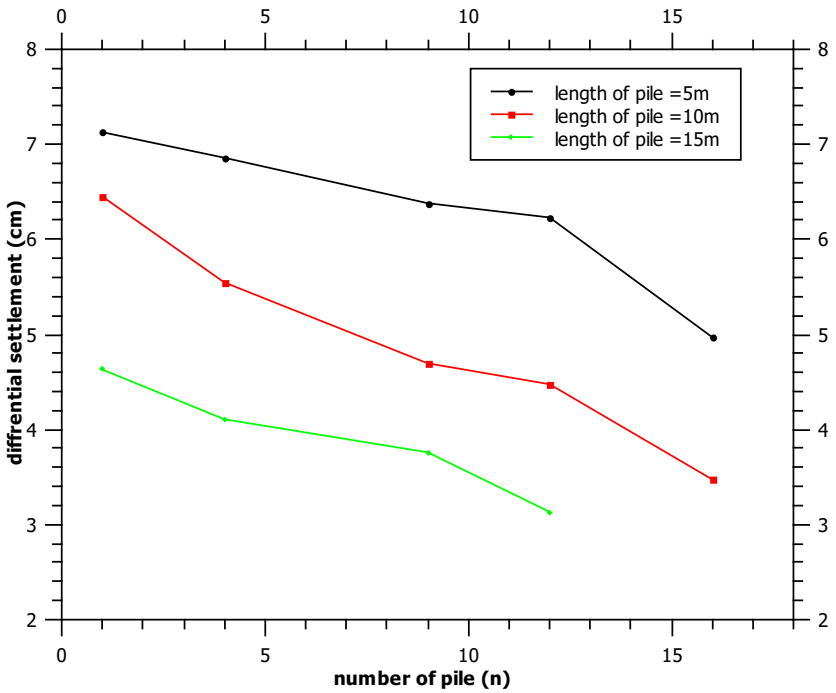

Figure 4.6: Differential settlement variations with number of pile

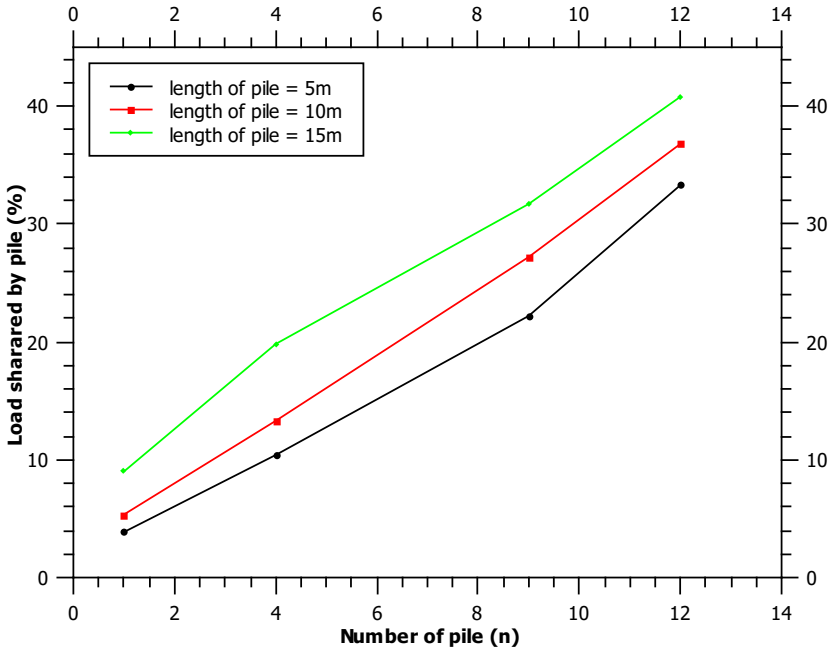

Figure 4.7: Load capacity variation with number of pile and length

vertical settlement decrease of 12 and 30mm is obtained for pile length increase to 10 and 15m respectively from the initial 5m pile length. And a differential settlement decrease of 15 and 30mm is obtained for the same length increment mentioned above which are significant figure in-terms of differential settlement. This behavior is attributed to the in-

crease in stiffness of the piled raft due to increase in pile length. From the above results, one can see pile length is a powerful parameter in settlement control.

The load sharing ratio, as defined in equation 2.23, is one way of evaluating the effectiveness of a piled raft foundation. Generally, an increase in load sharing ratio is observed with an increase in pile length, as confinement due to overburden pressure enhances the skin resistance capacity of the pile. Moreover, steep slope is observed with an increase in pile number due to variation in the rate of increase in load sharing ratio with a successive increase in pile number, i.e 6, 10, and 12% increase in load sharing ratio is obtained when a pile number increases from one to four, four to nine and nine to twelve respectively. A maximum load sharing ratio of 34 and 40.8% are obtained corresponding to the 12m pile. Hence, pile length is an important parameter in enhancing the load sharing ratio together with settlement control. Horikoshi and Randolph (1998) pointed out that using fewer long piles near the center are far more effective in settlement control and load sharing improvement than using many short piles. By providing a pile group over the central 26%(by area) of the raft, the piles carry 40% of the total load. This strategic use of piles was also reported by O'Brien et al. (2012).

Despite the usual practice of using similar pile length throughout the pile group area, the potential advantage of using staggered pile length is studied by Leung et al. (2010). The variation of pile length is described by pattern function which consists of linear and quadratic terms but limited to square pile groups. This study addresses the potential application of this concept to non-squared pile groups. The settlement performance of these pile length configurations is compared with previously studied similar pile length configurations. Although one can think of a plentiful pile length variations, these study attempts to investigate five practical pile length configuration shown in Fig.4.8. For a meaningful comparison of each, the total pile length is kept constant, 180m , while the model boundaries are manipulated according to the pile length variations. To achieve a similar pile length for each pile length configuration, the pile tip is varied according to a linear and parabolic pattern function given as in the subsequent equation below (in order of appearance on Fig. 4.8).

$$L(i) = 2.0833 * S(i) - 20 \tag{4.1}$$

$$L(i) = 1.3021 * S(i)^2 - 20 \tag{4.2}$$

$$L(i) = 4.685 * S(i) - 22.5 \tag{4.3}$$

$$L(i) = -2.0833 * S(i) - 10 \tag{4.4}$$

$$L(i) = -4.68875 * S(i) \tag{4.5}$$

where: S is spacing of pile from the center pile

i pile number from center pile

The differential settlement of each staggered pile length configuration normalized with that of differential settlement of similar pile length plot is shown in Fig. 4.9. It shows the potential advantage of using non-uniform pile length beneath the raft except pile length configuration 1, where longer piles are located at the center and decrease linearly towards the raft edge. The others have a normalized differential settlement ratio below one, which is beneficial. The observed behavior is due to a decrease in interaction effects of dissimilar pile length configurations.

Fig. 4.8 shows the schematic diagram of varying pile length configurations in order of increasing differential settlement performance of the piled raft foundation system. And Fig 4.9 reveals the differential settlement can be further suppressed nearly by half if we adopt pile length configuration 5. This has some practical application on sensitive structures such as nuclear power plants and machine foundations in which a lower differential settlement is anticipated.

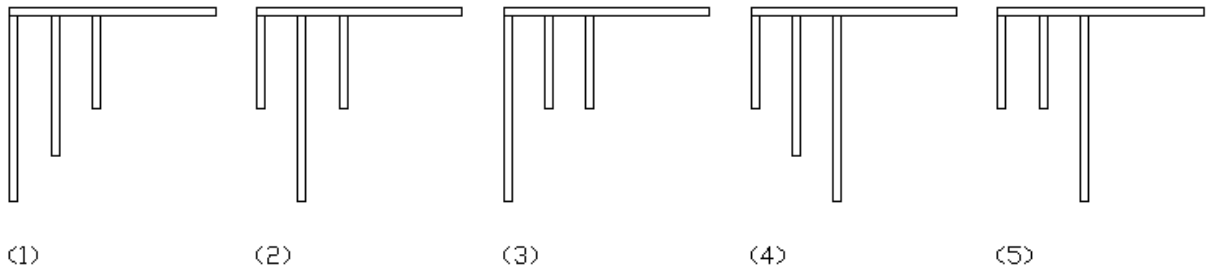

Figure 4.8: Staggered pile length configeration

4.2.3 Effect of pile spacing

The effect of pile spacing is investigated on a piled raft model of twelve piles having a length of fifteen meters. The spacing between piles is then varied as 3, 4, and 5 times the pile diameter. The finite element computational results are shown in Fig. 4.10.

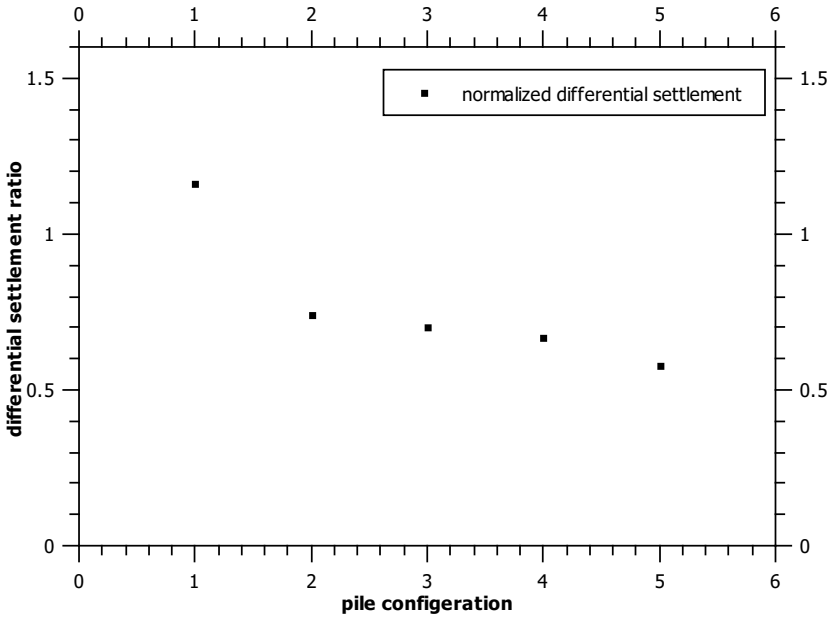

Figure 4.9: Normalised differentail settlement versus pile length

One reason for a decrease in vertical settlement for widely spaced piles is a reduction in interference among piles (stress overlap) that is to say for closely spaced piles the stress overlap area will be large leading to higher settlement. Vertical settlement reduction by 10mm is obtained with an increase in pile spacing from 3 to 5 times the pile diameter.

The differential settlement increases with an increase in pile spacing as widening the piles will reduce the central pile group stiffness. The computations show a maximum and minimum settlement occurs in the middle and edge areal portion of the raft and stiffening the area which results in maximum settlement (middle portion) with closely spaced piles is an ideal solution. Hence, a pile spacing of 3 times the diameter will give a reduced differential settlement which reveals a 20mm lesser differential settlement obtained from the spacing of 5 times the pile diameter.

Figure 4.11 shows an increase in load sharing by 4 and 10% with an increase in pile spacing to 4 and 5 times the pile diameter respectively. Mali and Singh (2020) studied the effect of pile length and spacing on soft and stiff clayey soils and found these two parameters considerably affects the load sharing capacity of the pile in piled raft foundation. They concluded that for any soil profile α_{pr} increases linearly as the spacing between piles increases. Similar Finite Element analysis was carried out by Sinha (2013) showing an

increase in differential settlement of piled raft foundation with an increase in spacing.

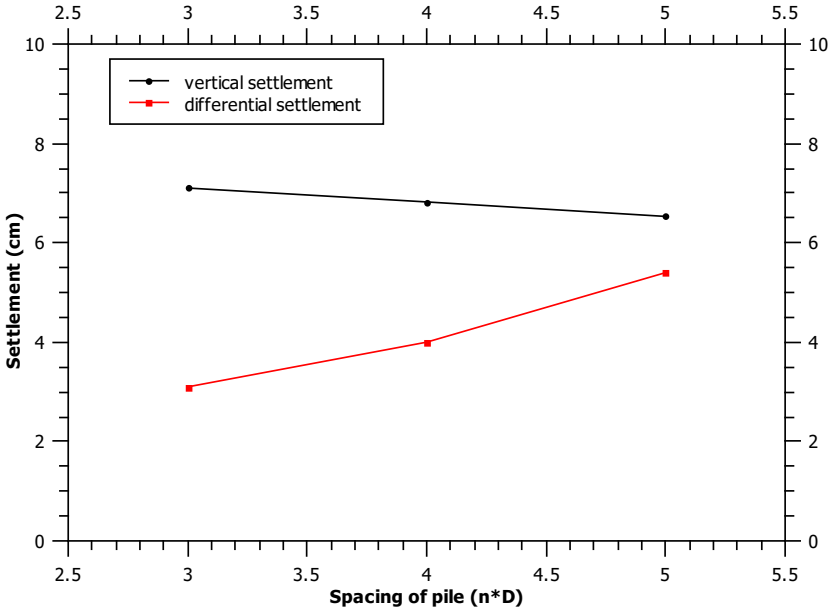

Figure 4.10: Settlement variation with pile spacing

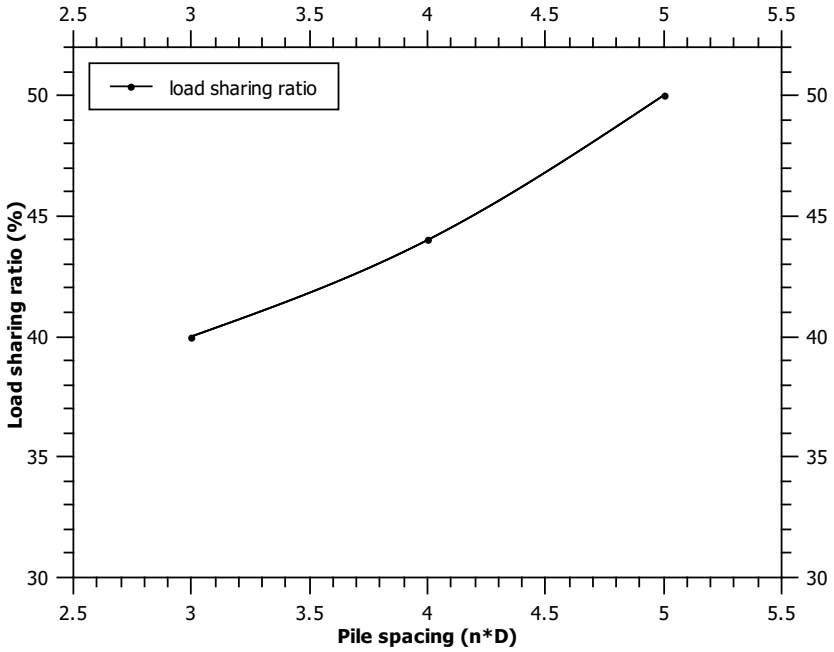

Figure 4.11: Load sharing ratio variation with pile spacing

4.2.4 Effect of pile diameter

The pile diameter is observed to be a less sensitive variant in-terms of settlement control (Figure 4.12). As clearly seen in Figure the vertical and differential settlement increases with 28 and 12mm by doubling the pile diameter. Although the pile load sharing capacity might increases significantly with an increase in pile diameter for end-bearing piles tipped on hard stratum.

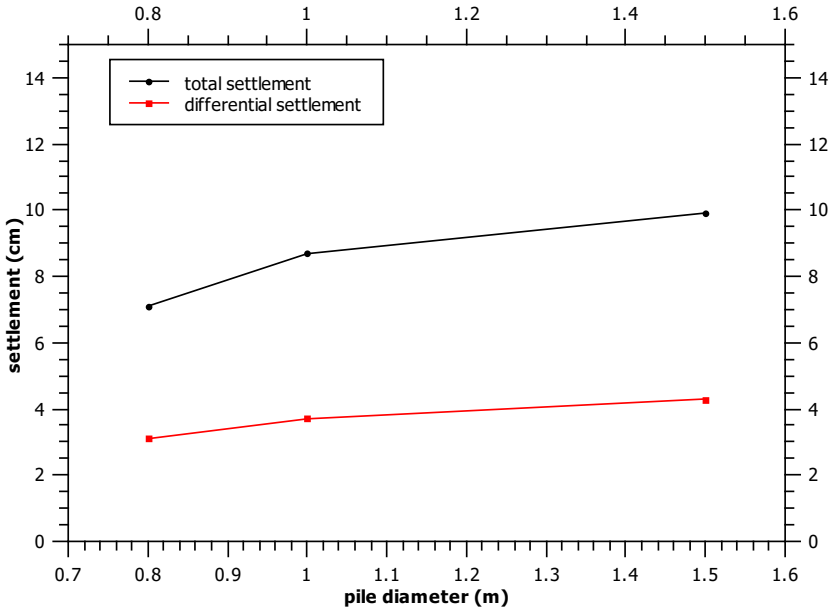

Figure 4.12: Settlement variation with pile diameter

4.2.5 Effect of consolidation

The long terms settlement and load sharing behavior of the pile raft foundation study is analyzed with a finite element model. The analysis was made on our basis piled raft layout (twelve piles of length fifteen) and we obtain an increase in vertical settlement (20mm) when a consolidation step is activated. The soil was allowed to drain in all the sides except the symmetry. The load carried by the pile was increased from 40.8 to 54 percent owing to blunt contact pressure and increased horizontal stresses around the pile. This indicates the designer shall consider the long term behavior of the piles when they are placed in clay soils. Also the usual practice of proportioning the super structural load to the pile and raft may yield erroneous results as the long term performance of these foundation

units will be altered due to consolidation effects. Reul and Randolph (2003) studied the effect of consolidation on clay soils on three performance indicators: maximum vertical and differential settlement and load sharing ratio of the piled raft foundations and they reported the effect of consolidation increase the proportion of the load carried by the pile up to 30%.

Chapter 5

Conclusion and Recommendation

5.1 Conclusion

The analyzed system consists of double symmetry square raft which has dimensions of 15 x 15m and a raft thickness of 0.7m. The number of piles with their respective length needed to meet the settlement requirement was determined first and these parameters are further kept constant to investigate the effect of other variants. Based on the numerical studies using Finite Element based software, computations can be summarized as follows:

- This study adopts a trial and error method to determine the adequate number of piles to meet the tolerable settlement value
- Increasing the pile number beyond a certain value is unnecessary and uneconomical.
- The increase in pile length decreases the vertical and differential settlement of the pile raft foundation while load sharing ratio is increased.
- The increase in pile spacing will decrease the vertical settlement while the differential settlement increases.
- The effect of pile diameter is insignificant in settlement control.
- By providing a pile group over the central 26% (by area) of the raft, the piles carry 40% of the total load.
- For the considered piled raft configuration, using dissimilar pile length layout, consecutive shorter piles near the center and longer at edges, improved the settlement performance of the pile raft foundation.
- Consolidation effects are investigated and an increase in vertical settlement by 20mm and load sharing ratio by 14% are observed.

5.2 Recommendation

Though this study is limited in its scope, the author hopes this will pave a way for settlement based approach analysis and design of piled raft foundation. For further improvement in designing a piled raft foundation the following recommendations are presented:

- The present work is limited to square pile rafts and further research should be conducted by varying the aspect ratio of the system.
- Interface behavior among the foundation units and between layers should be conducted to address the practical scenario.

Bibliography

OA Abdel-Azim, K Abdel-Rahman, and YM El-Mossallamy. Numerical investigation of optimized piled raft foundation for high-rise building in germany. *Innovative Infrastructure Solutions*, 5(1):1–11, 2020.

John R Booker and JC Small. Finite layer analysis of viscoelastic layered materials. *International Journal for Numerical and Analytical Methods in Geomechanics*, 10(4): 415–430, 1986.

LE Bowles et al. *Foundation analysis and design*. McGraw-hill, 1996.

RBJ Brinkgreve, E Engin, and WM Swolfs. Plaxis 3d 2013 user manual. *Plaxis bv, Delft*, 2013.

JB Burland. Piles as settlement reducers. In *The 8th Italian Conference on Soil Mechanics*, 1995.

R Butterfield and PK Banerjee. The problem of pile group–pile cap interaction. *Geotechnique*, 21(2):135–142, 1971.

Wai-Fah Chen, E Mizuno, et al. *Nonlinear analysis in soil mechanics*. Number BOOK. Elsevier Amsterdam, 1990.

Helen Sze Wai Chow. *Analysis of piled-raft foundations with piles of different lengths and diameters*. PhD thesis, University of Sydney, 2007.

P Clancy and MF Randolph. An approximate analysis procedure for piled raft foundations. *International Journal for Numerical and Analytical Methods in Geomechanics*, 17(12):849–869, 1993.

WGK Fleming. A new method for signle pile settlement prediction and analysis. *Geotechnique*, 42(3):411–425, 1992.

E Franke. Measurements beneath piled rafts. In *W: Key note lecture to the ENPC Conf. on Deep Foundations, Paris*, pages 1–28, 1991.

Eberhard Franke, Bernd Lutz, and Yasser El-Mossallamy. Measurements and numerical modelling of high rise building foundations on frankfurt clay. In *Vertical and Horizontal Deformations of Foundations and Embankments*, pages 1325–1336. ASCE, 1994.

Henok Fikre Gebregziabher and Martin Achmus. Influence of raft rigidity for piled rafts resting on stratified subsoil. *International Journal of Geotechnical Engineering*, 0(0):1–8, 2020. doi: 10.1080/19386362.2020.1809839. URL `https://doi.org/10.1080/19386362.2020.1809839`.

K Horikoshi and MF Randolph. On the definition of raft—soil stiffness ratio for rectangular rafts. *Géotechnique*, 47(5):1055–1061, 1997.

K Horikoshi and MF Randolph. A contribution to optimum design of piled rafts. *Geotechnique*, 48(3):301–317, 1998.

R Katzenbach, U Arslan, Chr Moormann, and O Reul. Piled raft foundation: interaction between piles and raft. *Darmstadt Geotechnics*, 4(2):279–296, 1998.

Fumio Kuwabara. An elastic analysis for piled raft foundations in a homogeneous soil. *Soils and foundations*, 29(1):82–92, 1989.

Poul V Lade. Overview of constitutive models for soils. In *Soil constitutive models: Evaluation, selection, and calibration*, pages 1–34. 2005.

YF Leung, A Klar, and K Soga. Theoretical study on pile length optimization of pile groups and piled rafts. *Journal of geotechnical and geoenvironmental engineering*, 136 (2):319–330, 2010.

Jerry P Love. The use of settlement reducing piles to support a flexible raft structure in west london. In *BGA International Conference on Foundations: Innovations, observations, design and practice: Proceedings of the international conference organised by British Geotechnical Association and held in Dundee, Scotland on 2–5th September 2003*, pages 531–540. Thomas Telford Publishing, 2003.

Shivanand Mali and Baleshwar Singh. 3d numerical modeling of large piled-raft foundation on clayey soils for different loadings and pile-raft configurations. *Studia Geotechnica et Mechanica*, 42(1):1–17, 2020.

Alessandro Mandolini, Gianpiero Russo, and Carlo Viggiani. Pile foundations: Experimental investigations, analysis and design. In *Proceedings of the International Conference on Soil Mechanics and Geotechnical Engineering*, volume 16, page 177. AA BALKEMA PUBLISHERS, 2005.

A.S. O'Brien, John Burland, and T. Chapman. Rafts and piled rafts. *ICE manual of geotechnical engineering*, 2:853–886, 01 2012.

Harry George Poulos and Edward Hughesdon Davis. *Elastic solutions for soil and rock mechanics*. Number BOOK. John Wiley, 1974.

HG Poulos. Analysis of piled strip foundations. In *International conference on computer methods and advances in geomechanics. 7*, pages 183–191, 1991.

HG Poulos. 16. practical design procedures for piled raft foundations. *Design applications of raft foundations. Thomas Telford Publishing*, pages 425–467, 2000.

HG Poulos. Piled raft foundations: design and applications. *Geotechnique*, 51(2):95–113, 2001.

Widjojo A Prakoso and Fred H Kulhawy. Contribution to piled raft foundation design. *Journal of Geotechnical and Geoenvironmental Engineering*, 127(1):17–24, 2001.

Mark F Randolph and C Peter Wroth. Analysis of deformation of vertically loaded piles. *Journal of Geotechnical and Geoenvironmental Engineering*, 104(ASCE 14262), 1978.

MF Randolph. Design of piled foundations. *Cambridge Univ. Eng. Dept*, 1983.

MF Randolph. Design methods for pile groups and piled rafts. In *International conference on soil mechanics and foundation engineering*, pages 61–82, 1994.

O Reul and MF Randolph. Piled rafts in overconsolidated clay: comparison of in situ measurements and numerical analyses. *Geotechnique*, 53(3):301–315, 2003.

Oliver Reul and Mark F Randolph. Design strategies for piled rafts subjected to nonuniform vertical loading. *Journal of Geotechnical and Geoenvironmental Engineering*, 130 (1):1–13, 2004.

Anup Sinha. *3-D modeling of piled raft foundation*. PhD thesis, Concordia University, 2013.

Alec Westley Skempton and Donald Hugh MacDonald. The allowable settlements of buildings. *Proceedings of the Institution of Civil Engineers*, 5(6):727–768, 1956.

JC Small and HH Zhang. Behavior of piled raft foundations under lateral and vertical loading. *International journal of geomechanics*, 2(1):29–45, 2002.

Stephen Timoshenko, S Timoshenko, and JN Goodier. *Theory of Elasticity, by S. Timoshenko and JN Goodier,...* McGraw-Hill book Company, 1951.

L Zeevaert. Compensated friction-pile foundation to reduce the settlement of buildings on the highly compressible volcanic clay of mexico city. In *Proc. 4th Int. Conf. on SMFE*, volume 1, pages 81–86, 1957.

Appendices

Chapter A

Limiting values of structural deformation and foundation movement

The components of foundation movement, which should be considered include settlement, rotation, tilt, relative deflection, relative rotation, horizontal displacement and vibration amplitude. Definition of some terms for foundation movement and deformation are given in Fig. For normal structures the local building code (ES EN-7) recommends use of total settlement up to 50mm for isolated foundations and a maximum acceptable relative rotations for sagging mode is 1/500 for many structures.

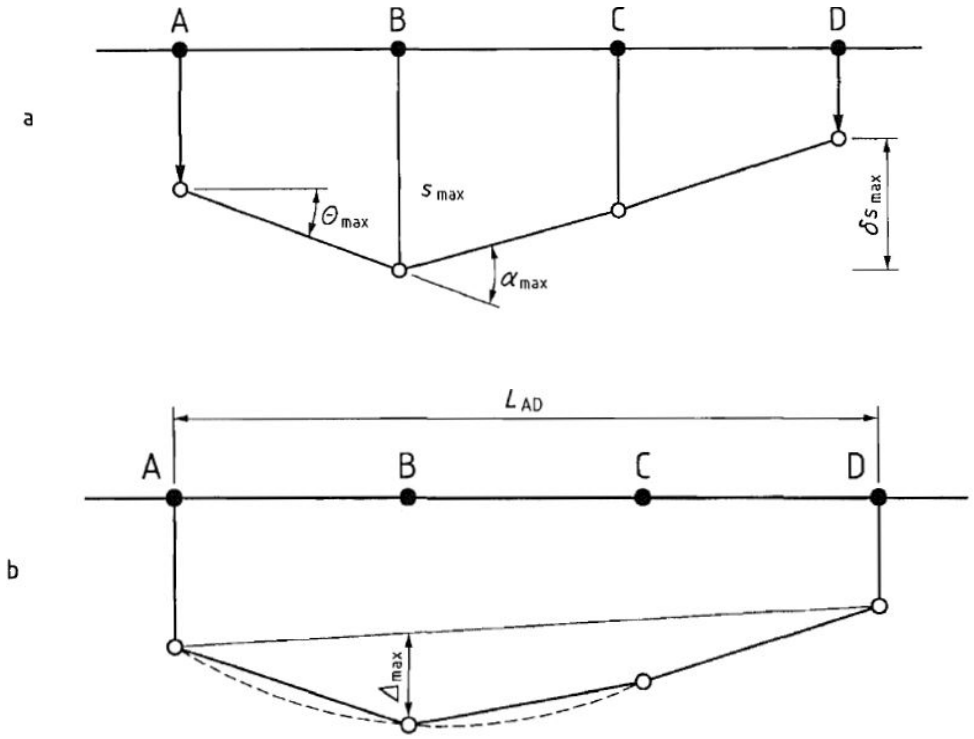

a) definition of settlement s,differential settlement δ_s, rotation θ and angular strain α

b) definition of relative deflection δ and deflection ratio δ/L

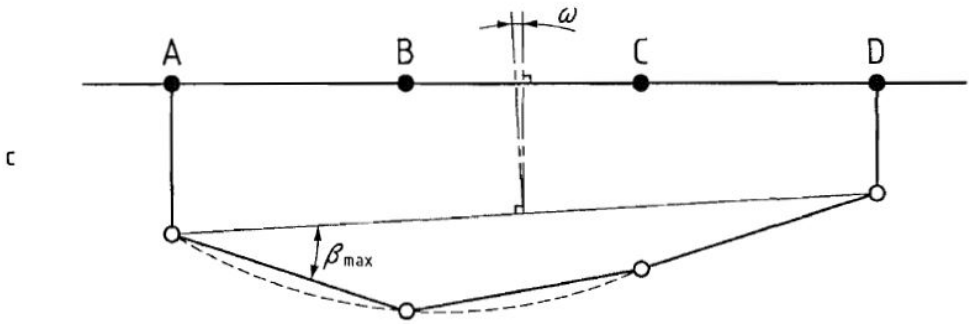

Figure A.1: Definition of foundation movements

Table A.1: Tolerable differential settlement of buildings, mm*

Criterion	Isolated foundations	Rafts
Angular distortion (cracking)	1/300	
Greatest differential settlement		
Clays	45(35)	
Sands	32(25)	
Maximum settlement		
Clays	75	$75 - 125(65 - 100)$
Sands	50	$50 - 75(35 - 65)$

After Macdonald and Skempton

c) definition of tilt ω and relative rotation (angular distortion) β

Bowles et al. (1996) recommendations are summarized in Table A.1.

Chapter B

Material model and structural behavior of foundation units

B.1 3D Plates

The plaxis 3D program allows for orthotropic material behavior in plate elements, which is defined by the following parameters:

E_1: Young's modulus in first axial direction

E_2: Young's modulus in second axial direction

G_{12}: In-plane shear modulus

G_{13}: Out-of-plane shear modulus related to shear deformation over first direction

G_{23}: Out-of-plane shear modulus related to shear deformation over second direction

ν_{12}: Poissons's ratio

The material behavior in plate elements is defined by the following relationship between strains and stresses, which is based on the general three dimensional continuum mechanics theory and the assumption that σ_{33}=0

$$\begin{bmatrix} \varepsilon_{11} \\ \varepsilon_{22} \\ \gamma_{12} \\ \gamma_{13} \\ \gamma_{23} \end{bmatrix} = \begin{bmatrix} \frac{1}{E_1} & \frac{-\nu_{12}}{E_1} & 0 & 0 & 0 \\ \frac{-\nu_{12}}{E_1} & \frac{1}{E_2} & 0 & 0 & 0 \\ 0 & 0 & \frac{1}{G_{12}} & 0 & 0 \\ 0 & 0 & 0 & \frac{1}{kG_{13}} & 0 \\ 0 & 0 & 0 & 0 & \frac{1}{kG_{23}} \end{bmatrix} = \begin{bmatrix} \sigma_{11} \\ \sigma_{22} \\ \sigma_{12} \\ \sigma_{13} \\ \sigma_{23} \end{bmatrix} \tag{B.1}$$

Inverting the relationship and ignoring higher order terms in ν gives:

$$\begin{bmatrix} \sigma_{11} \\ \sigma_{22} \\ \sigma_{12} \\ \sigma_{13} \\ \sigma_{23} \end{bmatrix} = \begin{bmatrix} E_1 & \nu_{12}E_2 & 0 & 0 & 0 \\ \nu_{12} & E_2 & 0 & 0 & 0 \\ 0 & 0 & G_{12} & 0 & 0 \\ 0 & 0 & 0 & kG_{13} & 0 \\ 0 & 0 & 0 & 0 & kG_{23} \end{bmatrix} = \begin{bmatrix} \varepsilon_{11} \\ \varepsilon_{22} \\ \gamma_{12} \\ \gamma_{13} \\ \gamma_{23} \end{bmatrix} \tag{B.2}$$

k is the shear correction factor, which is taken as $\frac{5}{6}$

B.2 3D Embedded Pile

An embedded pile in PLAXIS 3D consists of beam elements with embedded elements with embedded interface elements to describe the interaction with the soil at the pile skin and at the pile foot (bearing capacity). The material parameters of the embedded pile distinguish between the parameters of the beam and the parameters of the skin resistance and foot resistance. The beam elements are considered to be linear elastic and are defined by the same material parameters as a regular beam elements.

The interaction of the piles with the soil at the skin of the pile is described by linear elastic behavior with a finite strength and is defined by the following parameter:
T_{max}: Maximum traction allowed at the skin of the embedded pile (can vary along the pile)
The constitutive equation at the skin of the pile is defined by (Fig.8)

$$\begin{bmatrix} t_s \\ t_n \\ t_t \end{bmatrix} = \begin{bmatrix} K_s & 0 & 0 \\ 0 & K_n & 0 \\ 0 & 0 & K_t \end{bmatrix} = \begin{bmatrix} u_s^p - u_s^s \\ u_n^p - u_n^s \\ u_t^p - u_t^s \end{bmatrix} \tag{B.3}$$

where u^p denotes the displacement of the pile and u^s denotes the displacement of the soil. K_s denotes the elastic shear stiffness (againist parallel displacement differences) of the embedded interface elements and K_n and K_t denote the elastic normal stiffness (againist perpendicuar displacement difference) of the embedded interface elements. By default these values are defined such that the stiffness of the embedded interface elements does

not influence the total elastic stiffness of the pile-soil interaction:

$$K_s >> G_{soil}$$

$$K_n = K_t = \frac{2(1-\nu)}{1-2\nu} K_s \tag{B.4}$$

The normal stresses t_n and t_t will always remains elastic. For the shear stress in axial

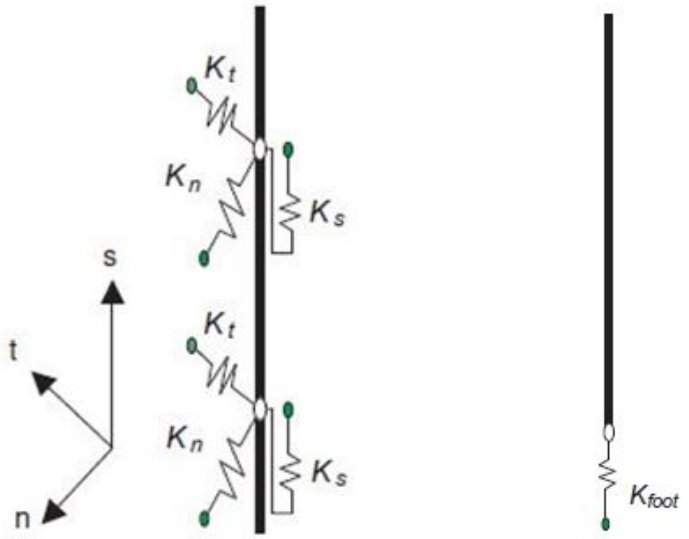

Figure B.1: Stiffness of the embedded interface elements at the skin and foot of the pile

direction t_s to remain elastic it is given by:

$$|t_s| < T_{max} \tag{B.5}$$

For plastic behavior the shear force t_s is given by:

$$|t_s| = T_{max} \tag{B.6}$$

In case of defining a layer dependent skin resistance the shear force t_s will remain elastic as long as:

$$|t_s| = (\sigma_n^{avg} tan\varphi_i + c_i)\pi D \qquad \text{and} \qquad |t_s| < T_{max} \tag{B.7}$$

where D denotes the diameter of the equivalent diameter (in the case alternative beam properties have been specified) of the embedded pile and σ_n^{avg} is the average lateral (per-

pendicular) stress of the soil around the pile:

$$\sigma_n^{avg} = \frac{1}{2}(\sigma_{xx} + \sigma_{yy}) \tag{B.8}$$

The paramaters φ_i and c_i are the friction angle and cohesion of embedded interfaces. The strength properties of embedded interfaces with layer dependent skin resistance are linked to the strength properties a soil layer. Each data set has an associated strength reduction factor for interfaces R_{inter}. The embedded interface properties are calculated from the soil properties in the associated data set and the strength reduction factor by applying the following rules:

$$tan\varphi_i = R_{inter} tan\varphi_{soil}$$

$$c_i = R_{inter} c_{soil} \tag{B.9}$$

For plastic behavior t_s is given by:

$$|t_s| = (\sigma_n^{avg} tan\varphi_i + c_i)\pi D \quad \text{provided that} \quad (\sigma_n^{avg} tan\varphi_i + c_i)\pi D \leq T_{max} \tag{B.10}$$

In the case of a layer dependent skin resistance where the actual bearing capacity is not known, T_{max} can be used as an ultimate cut-off value. The interaction of the pile with the soil at the foot of the pile is described by a linear elastic perfectly plastic interface elements. The strength of the base is described by the following parameters:
F_{max}: Maximum force allowed at the foot of the embedded pile
In addition, no tension forces are allowed. The constitutive relationship at the foot of the pile and its failure criterion are defined by:

$$F_{foot} = K_{foot}(u_{foot}^p - u_{foot}^s) < F_{max} \tag{B.11}$$

Where K_{foot} denotes the stiffness of the spring which is defined in the same way as the stiffness of the embedded interface elements:

$$K_{foot} >> G_{soil} \tag{B.12}$$

Table B.1: Properties of embedded pile

Description	Unit	Value/type
Young's modulus, E	kN/m^2	$3.5 * 10^7$
Unit weight, γ	kN/m^2	5
Type of pile	-	embedded pile
Diameter, d	m	0.8
Skin resistance distribution	-	layer dependent
T_{top}	kN/m^2	varying with depth
T_{bottom}	kN/m^2	varying with depth
Base resistance, F_{base}	kN	varying with depth

where skin and base resistance of the pile is computed using:

$$Q_s = \sum \alpha C_u P \Delta L, \alpha = 1 \tag{B.13}$$

$$Q_p = 9 C_u A_p \tag{B.14}$$

In the case of plastic behavior, the foot force F_{foot} is given by:

$$f_{foot} = F_{max} \tag{B.15}$$

In order to ensure that a realistic pile bearing capacity as specified can actually be reached, a zone in the soil volume elements surrounding the beam is identified where any kind of soil plasticity is excluded (elastic zone).

Chapter C

Element Formulation

C.1 Interpolation functions and numerical integration of volume elements

The soil volume in the PLAXIS program is modeled by means of 10-node tetrahedral elements. The interpolation functions, their derivatives and the numerical integration of this type of element are described in the following subsections.

C.1.1 10-node tetrahedral element

The 10-node tetrahedral elements are created in the 3D mesh procedure. This type of element provides a second-order interpolation of displacements. For tetrahedral elements there are three local coordinates (ξ, η, ζ). The shape functions N_i have the property that the function value is equal to unity at node i and zero at other nodes. The shape functions of these 10-node volume elements can be written as:

$$N_1 = (1 - \xi - \eta - \zeta)(1 - 2\xi - 2\eta - 2\zeta)$$

$$N_2 = \zeta(2\varsigma - 1)$$

$$N_3 = \xi(2\xi - 1)$$

$$N_4 = \eta(2\eta - 1)$$

$$N_5 = 4\zeta(1 - \xi - \eta - \zeta)$$

$$N_6 = 4\xi\zeta$$

$$N_7 = 4\xi(1 - \xi - \eta - \zeta)$$

$$N_8 = 4\eta(1 - \xi - \eta - \zeta)$$

Table C.1: 4-point integration for 10-node tetrahedral element

Point	ξ_i	η_i	ζ_i	w_i
1	$\frac{1}{4} - \frac{1}{20}\sqrt{5}$	$\frac{1}{4} - \frac{1}{20}\sqrt{5}$	$\frac{1}{4} - \frac{1}{20}\sqrt{5}$	$\frac{1}{24}$
2	$\frac{1}{4} - \frac{1}{20}\sqrt{5}$	$\frac{1}{4} - \frac{1}{20}\sqrt{5}$	$\frac{1}{4} + \frac{3}{20}\sqrt{5}$	$\frac{1}{24}$
3	$\frac{1}{4} + \frac{3}{20}\sqrt{5}$	$\frac{1}{4} - \frac{1}{20}\sqrt{5}$	$\frac{1}{4} - \frac{1}{20}\sqrt{5}$	$\frac{1}{24}$
4	$\frac{1}{4} - \frac{1}{20}\sqrt{5}$	$\frac{1}{4} + \frac{3}{20}\sqrt{5}$	$\frac{1}{4} - \frac{1}{20}\sqrt{5}$	$\frac{1}{24}$

$$N_9 = 4\eta\zeta$$

$$N_10 = 4\xi\eta \tag{C.1}$$

The soil element have three degrees of freedom per node: u_x, u_y, and u_z. The shape

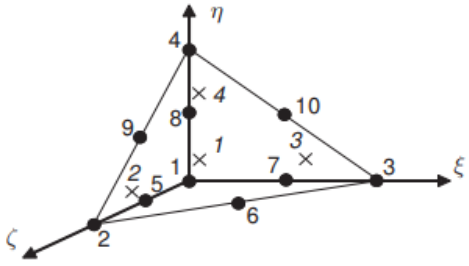

Figure C.1: Local numbering and positioning of nodes (•) and integration points (x) of a 10-node wedge element

function matrix $\underline{N_i}$ can be defined as:

$$\left[N_j\right] = \begin{bmatrix} N_i & 0 & 0 \\ 0 & N_i & 0 \\ 0 & 0 & N_i \end{bmatrix} \tag{C.2}$$

and the nodal displacement vector $\underline{v}$ is defined as:

$$v = [v_{ix} v_{iy} v_{iz}]^T \tag{C.3}$$

In order to calculate cartesian strain components from displacements derivates need to be taken with respect to the global system of axes (x, y, z).

C.1.2 Numerical integration over volumes

The numerical integration over volume can be formulated as:

$$\int\int\int F(\xi,\eta,\zeta)d\xi d\eta d\zeta \approx \sum_{i=1}^{k} F(\xi_i,\eta_i,\zeta_i)w_i \tag{C.4}$$

The PLAXIS program uses Gaussian integration within tetrahedral elements. The integration is based on 4 sample points. The position and weight factors of the integration points are given in Table 3.

C.1.3 Calculation of element stiffness matrix

The element stiffness matrix, K^e, is calculated by the integral:

$\underline{K^e}=\int \underline{B^T}\ \underline{D^e}\ \underline{\mathrm{B}}\ dv$

As it is more convenient to calculate the element stiffness matrix in the local coordinate system, the change of variable theorem should be applied to change the integral to the local coordinate system:

$\underline{K^e}=\int \underline{B^T}\ \underline{D^e}\ \underline{\mathrm{B}}\ jdV*$

where j denotes the determinant of the jacobian and the integral is estimated by numerical integration